Marine Geology
October 2020, Volume 428, Pages 106242 (29p.)
https://doi.org/10.1016/j.margeo.2020.106242
https://archimer.ifremer.fr/doc/00635/74689/

Seafloor morphology and sediments transfers in the mixed carbonated-siliciclastic environment of the Lesser Antilles forearc along Barbuda and St. Lucia

Seibert C. [1, *], Feuillet N. [1], Ratzov Gueorgui [2], Beck C. [3], Cattaneo Antonio [4]

[1] Université de Paris, Institut de physique du globe de Paris, CNRS, F-75005 Paris, France
[2] Géoazur, Université de Nice Sophia-Antipolis, CNRS, Observatoire de la Côte d'Azur, 250 rue Albert Einstein, 06560 Valbonne, France
[3] CNRS ISTerre, Université Savoie-Mont-Blanc, 73 376 Le Bourget du Lac, France
[4] IFREMER, Géosciences Marines, BP. 70, 29280 Plouzané, France

* Corresponding author : C. Seibert, email address : seibert@ipgp.fr

Abstract :

The Lesser Antilles arc is a mixed siliciclastic and carbonate active margin made of active volcanic and flat plio-quaternary carbonate islands. It was built as a result of a complex tectonic history at the slowly converging boundary between the American plates and the Caribbean plate. The sedimentary processes as a consequence of external forcing (earthquakes, volcanism, hurricanes) were rarely documented in such environment and are poorly understood. We exploited an exceptional dataset of high-resolution marine seafloor data acquired during the last 20 years in the northern part half of the Lesser Antilles forearc to document the sediment-transport processes. We achieved a detailed morpho-sedimentary study from multi-beam bathymetry, backscattering, and seismic profiles. Two areas could be characterized: 1) the “Rough Area”, along Barbuda to Guadeloupe carbonated islands, characterized by steep (up to 25°) slopes incised by short canyons, and deep basins controlled by major normal faults; 2) the “Channelized Area”, south of Guadeloupe and bordered by active volcanic islands and carbonate platforms, characterized by gentle slopes incised by long canyons. During sea-level high-stands, the sediments seem exported from the carbonate platform by hurricanes or density cascading but appear to settle at the shelf-edge and canyon heads. During sea-level low-stands, a connection may exist between onshore and offshore systems. However, this sediment supply appears not sufficient to generate canyon formation, likely shaped by regressive processes. Shelf breaks of the carbonate banks, platforms and submarine slopes are affected by sediment failures. Some may be associated to voluminous remobilizations and large mass transport deposits. Large earthquakes are likely the main processes in this area to remobilize sediments toward the deep forearc basins by triggering both slope failures and flushing of the canyon head.

Highlights

► Morpho-sedimentary study of Lesser Antilles forearc ► Two distinct morphological domains along the forearc (Rough and Channelized areas). ► Active sediment transfers through canyons and slope failures supply the deep basins. ► Tectonic and sea-level fluctuations control the sediment transfers. ► Isolated basins should mainly record co-seismic turbidites.

Keywords : Seafloor morphology, Backscatter, Submarine canyons, Landslides, Lesser Antilles arc

1. Introduction

In subduction zones, numerous studies have been carried out on sediment transfer in siliciclastic environments, focusing particularly on development and evolution of submarine canyons, such as eastern margin of New Zealand (Mountjoy et al., 2009; Micallef et al., 2014), Makran (Bourget et al., 2011), Taiwan (Lehu et al., 2015; Chiang and Yu, 2006), Japan (Noda et al., 2008), Cascadia (McAdoo et al., 1996) or Ecuador (Collot et al., 2019) and Colombia (Ratzov et al., 2012). However, little is known on the development and evolution of the turbiditic systems due to tectonic forcing in mixed siliciclastic-carbonate and carbonate environment because in the last decades, most of the studies based on high-resolution marine data have been performed along passive margins (e.g. Exon et al., 2005; Puga-Bernabéu et al., 2013; Mulder et al., 2012, 2019; Tournadour et al., 2017; Principaud et al., 2018). Only few studies were performed on modern mixed systems in active tectonics areas (Andresen et al., 2003; Jorry et al., 2010) and none in subduction contexts. Those studies have concluded that turbiditic activity is predominantly controlled by the relative sea-level fluctuations and carbonated production in shallow environment rather than by earthquake destabilizations (Andresen et al., 2003; Jorry et al., 2010).

The Lesser Antilles is an ideal target to investigate the link between tectonics and morphological evolution of a mixed sedimentary system because: 1) it was built at an active margin as a results of the subduction of American plates under the Caribbean plate, 2) as a result of a complex history of subduction processes (Bouysse and Guennoc, 1983), it is composed of two type of islands (active volcanic island and carbonate platform), 3) several studies were previously performed on the submarine domain in volcanology (Deplus et al., 2001; Le Friant et al., 2004; Trofimovs et al., 2010, 2013; Brunet et al., 2016) and tectonics

(Feuillet et al., 2002, 2004, 2011a; Leclerc et al., 2016) allowing to constrain the volcanic and tectonic chronologies. We are benefitting of an exceptional marine data set with resolution rarely attained in other volcanic arcs worldwide, and most active fault systems and submarine volcanoes have been described and documented at all scales. However, only few sedimentary studies have been carried out in the Lesser Antilles arc and most of them are in the back-arc domain, to characterize sedimentary deposits related to volcanic activity (Deplus et al., 2001; Le Friant et al., 2004; Picard et al., 2006; Trofimovs et al., 2010, 2013; Brunet et al., 2016) and active faulting (Beck et al., 2012). Additionally, only few sediment cores were collected in the forearc domain, along the slopes of the outer arc island, or above the subduction interface to investigate the regional-scale sedimentary processes (Wright, 1984; Reid et al., 1996). Without high-resolution marine data to document the turbiditic systems, this study was limited.

The main goal of this study is to improve the knowledge of sediment transfers and their forcing mechanisms along a subduction zone in carbonated and mixed siliciclastic-carbonate environments. In particularly, we aim to understand better the potential triggers of gravity flows and the associated deposits in the deep basins for further paleoseismological investigations in the framework of the CASEIS project (Feuillet, 2016, Seibert, 2019). Along such margin, large earthquakes may greatly influence the sedimentary processes. They can generate both disturbances in the sediments and submarine gravity currents (Heezen and Ewing, 1952; Montenat et al., 2007). Mountjoy et al. (2018) described notably the flushing of the canyon head through the deep environments triggered by the Mw 7.8 2016 Kaikura earthquakes (New Zealand). In mixed environment, however, such processes are still poorly documented due to lack of high-resolution data. We focused our study in the fore-arc domain, above the deep part of subduction interface offshore Guadeloupe and Martinique where the two largest M8 class historical earthquakes occurred on January 11 1839 and on February 8 1843 (Robson et al., 1964; Bernard and Lambert 1988, Feuillet et al., 2011, Hough 2013). Indeed, understanding all sediment transfer modalities is a must for subsequent tectonic and paleo-seismic studies based on sediment analyses.

The aims of this paper are to 1) figure the sediment transport toward the forearc basins, either from the shelves of volcanic and carbonate islands and banks, or from the accretionary prism, and 2) to discuss the influences of external forcing (Quaternary eustatic sea-level changes, tectonic movements related to the megathrust and active faulting) on these sedimentary processes. The analyses will be based on an important dataset of high-resolution

multibeam bathymetry, backscatter, and seismic reflection profile, to identify and map at ranges of scale the main canyons, slope failures scars, mass transport deposits (MTD), sediment bedforms, basins and faults.

2. Background

2.1. Geological setting of the Lesser Antilles Arc

The Lesser Antilles arc results from the subduction of the North and South American plates beneath the Caribbean Plate (Fig. 1A) in a ENE-WSW direction at a rate of 2 cm/yr (Deng and Sykes, 1995; DeMets et al., 2000; Symithe et al., 2015). It is 800 km-long, extending from the Anegada passage (between Puerto Rico and Virgin Islands) to the South American coast. To the north, the arc is separated by the NNW-SSE-striking, 250 km-long up to 1500 m-deep Kallinago through (Bouysse and Guennoc 1983) into two subparallel islands' alignments that splay from Martinique (Fig. 1). The western line is the inner active volcanic arc. It is made of a dozen of islands ("Volcanic Caribbees", South to North: Grenade, St. Vincent, St. Lucie, Martinique, Dominica, Basse-Terre - western part of Guadeloupe, Montserrat, Nevis, St. Kitts, St Eustarius and Saba islands; Fig 1B) and is active since the end of the Miocene (Andreieff et al., 1979; Bouysse et al., 1985; Bouysse and Westercamp, 1990; Bouysse and Mascle, 1994). The eastern line is the outer arc, which is made of old paleogene extinct volcanic complexes, now abraded and covered by Plio-Quaternary limestone platforms ("limestone Caribbees", South to North: Marie-Galante, Grande-Terre – eastern part of Guadeloupe, Antigua, Barbuda, St. Barth, St. Martin and Anguilla islands; Fig. 1B). Several submarine carbonate banks belong to the outer arc, such as Dien Bien Phu (DBP), Amerique, Bertrand and Falmouth banks (Fig. 1B). They are former volcanic guyots covered by carbonate (Bouysse et Guennoc, 1983; Münch et al., 2013). East of Grande-Terre, the Karukera spur is a Jurassic magmatic basement covered by a carbonate platform upon which has developed to the Flandre bank (Münch et al., 2013; De Min et al., 2015). The Karukera spur has experienced several phases of tectonic activity and is now tilted toward the south; the oldest formations of the spur emerge to the North at La Desirade island (Münch et al., 2013; De Min et al., 2015).

Westwards, the Lesser Antilles arc is separated from the Aves Ridge by the N.S.-elongated Grenada Basin (Fig. 1B). This basin is filled with about 9000 m of sediments (Pinet et al., 1985). Eastwards, the forearc morphology shows a latitudinal dissymmetry. North of the

Flandre Bank, it is characterized by several deep basins (Fig. 1B). The Caribbean basement crops out along the steep slopes of the deepest basins (Bouysse and Mascle, 1994). These basins are controlled by NE-SW normal faults with several thousands of meters high scarps (Feuillet et al., 2002), the most important being the Desirade scarp. Conversely, south of Karukera spur, the slope is more regular, dips gently and is covered by several hundreds of meters of sediment resting upon an older volcanic basement complex (Bouysse and Mascle, 1994).

The Barbados accretionary wedge, which is one of the most voluminous worldwide, extends between the forearc basins and the trench (Fig. 1). It has been built by accretion of sediment supplied from the Orinoco river, which drain the northern terrains of the South America continent since the Late Paleocene, mixed with *in situ* hemipelagic layers (Westbrook et al., 1982; Beck et al., 1990; Stéphan et al., 1990; Pindell et al., 2006; Deville and Mascle, 2012) during an eastward relative displacement of the Caribbean plate. Thus, this prism is much wider (240 km) and thicker (15 km) to the south. The imbricated sedimentary and tectonic mixing crops out in Barbados island (Speed, 1981). Within the southern half of the accretionary prism, huge mass transport deposits (MTDs) and mud diapirs have been attributed to gas hydrates occurrences (Ferguson et al., 1993; Deville et al., 2003). The eastern boundary of the prism is deformed by the subduction of the Barracuda, Tiburón and St. Lucia oceanic ridges (Westbrook et al., 1988; Bouysse and Westercamp, 1990; Bangs et al., 2003; Pichot et al., 2012; Evain et al., 2013, Laigle et al., 2013; Fig. 1B).

2.2. Seismo-tectonic context

Numerous earthquakes have been recorded and documented during the historical and instrumental periods (Robson, 1964; Sykes and Ewing, 1965; Dorel, 1981; Stein et al., 1982; Feuillard, 1985; Bernard and Lambert, 1988; Feuillet et al., 2011a, b). However, the seismicity is considered to be low for a subduction zone and is interpreted as a consequence of the low convergence rate (Stein et al., 1982, DeMets et al., 2000). Only two very damaging earthquakes have been reported, on January 11, 1839 and February 8, 1843 (Fig. 1B). They respectively destroyed the cities of Fort-de-France (Martinique) and Pointe-à-Pitre (Guadeloupe) and resulted in thousands of casualties. The source and magnitude of those earthquakes are still controversial. Bernard and Lambert (1988) and Feuillet et al. (2011a) interpreted these earthquakes as megathrust earthquakes. Bernard and Lambert (1988)

proposed a magnitude ranging between 7.5 and 8, whereas Robson (1964), Shepherd (1992), Feuillet et al. (2011a), and Hough, (2013) suggest a magnitude 8 + earthquakes.

The islands of the Lesser Antilles arc are struck by numerous intraplate earthquakes of moderate to high magnitudes (Mw 7.4 October 8, 1974 near Antigua; March 16, 1985 near Montserrat; Feuillet et al., 2011a). The most recent one occurred in November 21 2004 in Guadeloupe (M 6.3 Les Saintes earthquake; Bazin et al., 2010; Feuillet et al., 2011b; Fig. 1B). They were generated along intra-plate faults (Feuillet et al., 2001, 2004; Leclerc et al., 2014), interpreted as the result of slip-partitioning and extension perpendicular to plate convergence (Feuillet et al., 2001, 2011a). Two main families have been identified: 1) the normal faults perpendicular to the arc which bounding the graben and half graben of the forearc; and 2) a set of *en échelon* right stepping faults (Feuillet et al., 2010; Leclerc et al. 2014) which spread throughout all the island arc. Seismic activity along these faults influences the sedimentation processes at a local scale (Feuillet et al., 2001; Beck et al., 2012; Leclerc et al., 2014, 2016).

2.3. Current sedimentary sources and processes

The Lesser Antilles margin is fed by more or less distant sediments sources. The Orinoco river and southwards the Amazon river contribute to bring fine grained particles (clay, silt and fine sand) towards the southern part of the arc, transported by the Guyana Littoral Current (Reid et al., 1996; Warne et al., 2002; Fig. 1A). In addition, a part of sediment inputs of the Orinoco can reach the Puerto-Rico trench *via* a dense network of channels which runs against the southern border of the Barbados accretionary wedge at the tip the river's delta and then all converge in the Vidal deep-sea channel in the Mid-Atlantic Ocean (Embley et al., 1970; Deville et al., 2015; Fig. 1A). The African continent represents also an additional minor supplier through high altitude wind transport (Prospero et al., 1970, 2014; Yu et al., 2015).

At more regional scale, twenty-one active volcanoes located on eleven islands (Fig. 1B), characterized by explosive eruptions sometimes accompanied by dome extrusions (Lindsay et al., 2003; Carn et al., 2004) bring a lot of volcanoclastic material offshore (Sigurdsson et al., 1980; Carey and Sigurdsson, 1980; Sigurdsson and Carey, 1981; Carey and Sigurdsson, 1984; Hart et al. 2004). During eruptions, volcanic particles can be carried directly to the sea, like tephra-fall and pyroclastic flow. The tephra-fall deposits were documented in cores sampled on both sides of the arc (Sigurdsson and Carey, 1981; Reid et al., 1996; Picard et al., 2006; Le Friant et al., 2008), whereas pyroclastic flows were preferentially observed in the backarc area, in the Grenada basin (Picard et al., 2006). Between eruptions, volcanic sediment can be

transported toward the sea by secondary processes. Recent fallout deposits but also older volcanic rocks of the basement can be remobilized from the islands by erosion and transport either by winds or river flows. In tropical areas, where powerful storms and hurricanes occur, mechanical erosion is very strong and torrential regime of waterfalls can induce many landslides (Zahibo et al., 2007, Saffache et al., 2002, 2003; Rad et al., 2013). It seems that mechanical erosion is more important along the slopes of the most recent volcanic edifice (in Guadeloupe mean of 2555 t/km^2/yr; Rad et al., 2006, 2013). Finally, significant sedimentary source in the Lesser Antilles arc is carbonate production. It has two origins: shallow-water carbonate from carbonate platforms and pelagic carbonate from the open ocean surface (Reid et al.,1996). The outer arc islands are all surrounded by wide carbonate platforms, which are bringing a lot of carbonate sediment (Reid et al., 1996; Fig. 1B).

The sedimentation rates estimated in the area are low, between 2 to 10 cm/ky on both side of the arc (Reid et al., 1996; Le Friant et al., 2008) and 1.5 cm/ky in the abyssal plain (Moore et al., 1988). However, Beck et al. (2012) estimated a higher rate of 53 cm/ky for the historical period on the basis of ^{210}Pb concentration, in a basin located between Nevis and Montserrat. This much higher rate can be partly explained by the lower compaction of sediment near the seafloor interface and also by the position of the core in an intra-arc steep basin.

Submarine landslides which are either flank collapses of active volcanoes (Deplus et al., 2001; Le Friant et al., 2003, 2004; Boudon et al., 2007; Trofimovs et al., 2013; Fig. 1B), whose the materiel settled at the base of submarine flank (Brunet et al., 2016) or slope failure of carbonate platform (Le Friant et al., 2004; Trofimovs et al., 2010, 2013). Pumice-rich volcanoclastic debris-flow deposits and turbidites were observed in Grenada Basin (Picard et al., 2006). Reid et al. (1996) show that the sediments of carbonate platforms (i.e. volcanic and rich aragonite and Mg-calcite carbonate) can be exported toward deeper environments by plums or turbidity flows (Reid et al., 1996). The strong westerly current favors these expulsions toward the backarc (Reid et al., 1996; Johns et al., 2002).

There are several potential triggers for turbidity currents on the Lesser Antilles area: sea-level falls, storm waves, earthquakes, or volcanic activity, aerial and submarine slope failures (Reid et al., 1996; Picard et al., 2006; Trofimovs et al., 2013; Brunet et al., 2016). According to the sedimentary study of Reid et al. (1996), the turbidites are more frequent and thicker during the glacial periods, like siliciclastic environments and volcanic arcs. More recently, Beck et al. (2012) have identified and characterized a sedimentary event between Nevis and

Montserrat islands. They proposed that this layer was triggered either by the 1974 earthquake or by the 1985 earthquake.

3. Materials and Methods

3.1. Bathymetry

Numerous cruises were performed during the last 20 years. Used devices and navigation grids are summarized on table 1 and Appendix A. This led to an extensive unique dataset of highly detailed seafloor images. We construct a geographic information system project (with ESRI ArcGIS software) with all Digital Elevation Models (DEMs) issued from different cruises, gridded at 100 m of resolution with the projection WGS84 World Mercator with 15°30'N parallel reference. A high resolution but noisier bathymetric map gridded at 50 m was used to highlight smaller structures. For shallow areas, we could add two other different datasets: numeric chart of the French Marine by SHOM with a resolution of 50 m and LITTO3D campaign by IGN and SHOM with a very high resolution of 5 m from 0 to 10 m depth below sea level (Table 1). In areas not covered by high-resolution bathymetry, we used the open worldwide database available in GeoMapApp (http://www.geomapapp.org; Ryan et al., 2009), which includes high resolution (100 m) seabeam data from cruises and ASTER (Advanced Spaceborne Thermal Emission and Reflection Radiometer) and NED (National Elevation Datased) data. For the topography, we use the 30-m SRTM data (Shuttle Radar Topography Mission - NASA).

3.2. Acoustic backscatter

Reflectivity data from the EM12 sounder collected during the AGUADOMAR cruise (1999) on the R/V ATALANTE were processed with the "belle-image" treatment of IFREMER's CARAIBES software (Domzig et al., 2009), that attenuates the tracks of the navigation roads. Despite these corrections, the reflectivity data is still less resolved between Antigua and Guadeloupe island. The acoustic backscatter helps characterizing the nature of seafloor. It may be used to identify slope break (fault scarps), river beds and slopes of basins and gives information on induration, grain size and water content. We could distinguish several acoustic facies according to a qualitative characterization of the signal intensity and homogeneity. Nine acoustic facies have been identified, organized into four classes: very high, high, medium, low and very low reflectivity (Table 2; Fig. 2). A heterogeneous facies

defines a surface of an intensity which is disrupted by small shapeless-patches of a more or less reflectivity.

3.3. Seismic profiles

Two seismic profiles, processed with SEISMIC UNIX from the AGUADOMAR cruise (see details in Feuillet et al., 2004) are used to illustrate the geometry of the sedimentary units and of the faults at depth in the forearc of the Lesser Antilles. We also used sub-bottom (SB) profiles to bring constraints the architecture of specific sedimentary structures. Two profiles were acquired during the CASEIS cruise (Feuillet, 2016) and one profile during the GWADASEIS cruise (Feuillet, 2009) with a 2.8 to 5.1 kHz and a 1.8 to 5.3 kHz signal frequency, respectively. On both campaigns, the profiles were processed with MATLAB software and SEISMIC UNIX.

4. Results

4.1. Overall morphology of the Lesser Antilles Arc

Our dataset highlights at range of scales the main bathymetric features of the eastern border of the Caribbean plate (Fig. 1 and Appendix B). To the west, all the drainage systems coming from the South-America shelf, the western shelf of the Lesser Antilles inner arc and the eastern shelf of the Aves Ridge flow into the 3000 m-deep Grenada Basin (Fig. 1B). North of the basin, the morphology is characterized by four valleys that all spread between the western slope of the arc and the eastern slope of the Aves Ridge and have a NE-SW strike (along the main slope): 1) in front of St Kitts and Nevis, 2) between St Kitts and Montserrat, 3) between Montserrat and Guadeloupe and 4) offshore Basse-Terre of Guadeloupe (Fig. 1B). The later one named Pointe Noire valley is the common outlet of all steep canyons draining the western slope of the insular shelf of Basse Terre. Westward, the four valleys are connected to another N-S striking valley (Grenada valley), which runs along the east border of the Aves Ridge toward the Grenada Basin.

On the eastern side of the arc, three areas are distinguished (profile AA’’’; Fig. 1C). To the North, between the Anegada Passage and the Flandre Bank, the morphology of the seafloor is characterized by several SW-NE striking deep basins and valleys, up to 5800 m-deep (St Barthélémy valley, Antigua valley, Meduse basin and Desirade valley), bounded by NE-SW striking normal faults (Feuillet et al., 2002; Fig. 1B). These steep slopes are incised by

numerous straight and short canyons (Fig. 1B). South of the Flandre Bank, the gentler insular slope is disrupted by several long and well-developed canyons that all flow towards the NNW-SSE striking Martinique Basin. Further south, the Tobago Basin is parallel to the arc and has a maximum depth of 2500 m. It collects the sediments coming from the American platform as well as from the group of Grenadines islands (Fig. 1B). The Tobago Basin is separated from the Martinique Basin by a smooth relief that goes up to 1700 m-depth and is about 70 km-long (Fig. 1B).

4.2. The "Rough area" between Barbuda and La Desirade

The Rough area is located between Barbuda and La Desirade and comprises four islands located on the older and inactive outer arc (Fig. 3A). Barbuda and Antigua are surrounded by the Antigua-Barbuda carbonate platform, which is about 3,000 km^2, 25 m-deep, and up to 15 km wide (from the island coasts to the shelf break). The carbonate platform around Guadeloupe and La Désirade is smaller (2 km-wide, 1200 km^2) and lies between 20 and 30 m depth (Münch et al., 2013). Four bathymetric highs are observed. The Flandre Bank extends eastwards from La Desirade with an area of 35 km^2 and a 40 mbsl depth. The Falmouth (14 km^2, ~70 mbsl) and Bertrand banks (15 km^2, ~ 70 mbsl) are both located between Guadeloupe and Antigua. These three banks are carbonated platform. The deeper Meduse Mount (600 mbsl), eastward from Antigua, is highly reflective (Fig. 3B).

Downwards, the whole area shows a complex and rough bathymetry which is outlined by steep slopes reaching up to 26° and a 5000 m-height (Desirade valley and Desirade scarp). The area is mainly controlled by the linear, up to 60 km-long, normal faults identified and mapped by Feuillet et al. (2002, 2004; Figs. 3A and 4). These faults bound spurs and basins. The basins might either be perched on the slope (Falmouth between 900 and 1180 mbsl, Willoughby between 2130 and 3000 mbsl and Turtle between 2600 and 2860 mbsl valleys; Figs. 3A and 4) or at the toe of the slope (Desirade Half Graben, 5600 mbsl; Falmouth Half Graben, 5830 mbsl; Caravelle Half Graben, 5590 mbsl and Desirade Basin, 5710 mbsl, Meduse Basin 5500 mbsl, Antigua Valley 4050 mbsl; Figs. 3A and 4). To the East, the whole area is delimited by the reliefs that mark off the edge of the accretionary prism.

4.2.1. Guadeloupe – La Desirade: from narrow shelf and steep slopes to Desirade valley

The trough between the Desirade fault scarp and the Falmouth-Bertrand spur shows three main morphological domains (Fig. 3C): steep slopes on the arc basement (~15°), a valley floors dipping gently from 6 to 2° and, at their end, deep basins which are almost flat (Fig. 3). Thus, the Desirade valley concentrates all the sediment supply transiting along a ~30 km-wide amphitheater. Its southern side corresponds to the 40 km-long E-W trending linear Desirade fault scarp. The structure is north-westwards prolonged by the Grande-Terre (11°) and the Bertrand Spur (9°) slopes. These three main segments shows different morphologic characteristics (Fig. 5).

Desirade scarp steep slopes

The Desirade fault scarp is characterized by three distinct morphologies from East to West, cross-cut by numerous V-shaped straight canyons. The eastern Desirade scarp is characterized by a distinct steep upper slope, decreasing downstream from 25° to 18° (segment 1 on Fig. 5A), resulting in a lower reflectivity at the toe of the scarp. There, canyons are highly reflective (Fig. 5B). In its middle part (segment 2 on Fig. 5A), the scarp is incised by two major canyons, up to 500 mbsl (green and yellow; on Figs. 5A, 6A and 6B). Canyons are connected to the Desirade shelf break and Flandre Bank respectively (Fig. 5A). The eastern canyon (Yellow) is clearly rooted on a normal fault (Feuillet et al., 2004). Along the Desirade island, the scarp has the steepest slope gradient (26°) and canyons with ~100 m-deep incision (segment 3 on Fig. 5A,). Segments 2 and 3 canyons are not distinguished on the backscatter along the scarp which have a very high reflectivity (Fig. 5B). This contrasts with the very low reflectivity of the well-stratified sediment filling the basin at the base of the scarp (Fig. 4 and 5B). All canyons feed the Desirade valley (Fig. 5A). The mouth of the strongly-incised canyon along segment 2 (green canyon on Fig. 5B) reveals a lobe with a higher reflectivity.

Grande-Terre steep to medium slopes

Offshore the eastern coasts of Grande-Terre (Fig. 5A), three main dendritic drainage systems incise the shelf break, from South to North: the Salines, Mussel and Bark canyon systems. Their upper part is composed of numerous short tributaries (~ 2 km-long, 0.6 km-wide), connected to the shelf break (~ 120 m), merging downstream along the steep slope (Fig. 5A). Their cross-section geometry evolves downstream from a sharp V- to a U-shape

profile, with a transition occurring at ~ 1800 mbsl (Fig. 6C). The only exception, located between Saline and Mussel systems, is most likely rooted on a slope failure scar, since its thalweg is much larger (2.5 km-wide) and shows an arcuate shape (Fig. 5A). The Salines and Mussel systems show similar incisions. On the upper part, they are few tens of meters to ~ 250 m-deep while they are 200 to 500 m below 1000 mbsl. The Castle canyon, which head incises the carbonate shelf between La Desirade and Grande-Terre islands (Figs. 6A), is the most deeply incised (up to 600 m-deep; Fig. 6C). The seafloor of these canyons shows a very high reflectivity on their upper part and a high reflectivity downslope (Fig. 5B). To the North, the Bark system is less incised (up to 200 m; Fig. 6C) and evolves into a smoother slope (10°). Its thalweg is highly reflective (Fig. 5B). Its upper part is less reflective and less defined than the Mussel and Salines systems.

Among the described systems, other canyons with heads confined to the slope appear, either merging with the main systems or forming distinctive ones (represented in black on Fig. 5A). They are less incised (less than 100 m, red dashed lines on Fig. 6C) and lower reflective with respect to the larger dendritic systems (Fig. 5B). Two canyons of this set are remarkable: 1) the Merne canyon which is up to 400 m deep and shows a strongly V-shaped all along the slope (Fig. 6C); this canyon is unusual since it is located on top of a promontory, and it has a very linear shape (Fig. 6A), highlighted by a high reflectivity (Fig. 5B), it is therefore most likely rooted on a fault, and 2) a canyon characterized by an arched scar head not connected to the carbonate shelf (Fig. 6A), which is likely a slope failure scar. Several gullies prolong downstream this second canyon (dotted black circle on Figs. 6A and 6C), which does not exceed tens of meters of incision.

Bertrand spur: medium slope gradients

Downstream from the Bertrand spur, which is characterized by arched scars, the slope is divided into two areas of rough seafloor without distinctive drainage systems (Fig. 6A and 6C). Backscatter reveals two dendritic networks not visible on the bathymetry (Fig. 5B). These networks do not reach the top of the spur and present high reflective facies.

Desirade valley

Along the valley, where the slope gradient is gentle (progressive transition from 6 to 0°), two main structures are visible: 1) up to 640 m-large and very reflective blocks; and 2) bedforms on the seafloor with alternating higher and lower reflectivity (Figs. 5A and 5B). The latter sediment structures are arcuate and show two areas along stream (Figs. 5A and 6D). In

the upper part, where the mean slope is 1°, the mean values of the wavelength and crests height are 1.25 km and ~ 6 m, respectively while in the lower part where the slope is gentler (0.7°), these values are smaller (~ 4 m-high and 800 m-long).

4.2.2. Inter-islands carbonate reliefs to basins

Shallow area

Between Grande Terre and Antigua islands, the watershed limit (blue line on Fig 5C) runs near the Falmouth and Bertrand banks. The eastern rough area is thus only fed by sediment sources located eastwards from Antigua and Guadeloupe. This implies that no sediment is transported from the siliciclastic margin of the inner active volcanic arc into the basin of the rough eastern area. Several areas display a hummocky morphology and the slopes of the Falmouth and Bertrand banks are not channelized (Fig. 5C). We observe a similar morphology at the edge of the south-eastern Antigua shelf which is an area characterized by a mottled reflective facies in the backscatter (Fig. 5D, Table 2).

The Falmouth valley is currently not fed by any channelized system (Fig. 5C). The sediment filling of this valley is however discharged by three outlet areas: to the north towards Antigua Valley, and eastwards and southwards through the Willoughby and Bertrand canyons tributaries respectively. Between the Grande-Terre carbonate platform (GTP) and the Bertrand Bank (BB), the sediment is transported eastwards, and both feed the two other tributaries of the Bertrand canyon (Fig. 5C). Moreover, numerous slope failures account for the transfer through the canyon.

Willoughby and Bertrand canyon systems

The 60 km-long Bertrand and the 70 km-long Willoughby canyons share some similarities. They extend from Grande Terre to the Desirade valley and from Falmouth valley to the Falmouth Half graben respectively, with paths alternating steep slopes across the arc basement and gentle slopes streaming along the fault scarps base (Figs. 5C and 3D). They can be divided into five parts (numbered 1 to 5 on bathymetric and slope profiles on Fig. 3D).

1) **Flat Carbonated source.** Upstream from the incision of both canyon systems, the slope is gentle, corresponding to the Falmouth Valley and the Valley between the BB and the GTP. The area is not channelized (Fig. 5C), as evidenced on cross-section (Fig. 3D) and on the backscatter data (Fig. 5D).

2) **Convex-up incision.** The Bertrand Canyons system shows three main tributaries (Fig. 5C). Two come from the GTP and the BB respectively, and are oriented E-W. The third tributary comes from the Falmouth valley and shows a N-S direction. The Willoughby system is simpler, with only two tributaries, both originating in the Falmouth valley, along an E-W direction (Fig. 5C). Canyon heads are outlined by knickpoints located at 1100 and 1350 mbsl (Fig. 3D). Downstream, the profiles are convex-up (Fig. 3D) and outlined by a high reflectivity (Fig. 5D), the slope increases and then decrease gently (Fig. 3D). The cross sections reveal a V-shape with an up to 400 m-deep incision (Fig. 3D). This trend is observed down to 2700 and 2100 mbsl for the Bertrand and Willoughby canyon.
3) **Fault-bounded Flat.** The slopes flatten over distances of 12 km and 32 km for the Bertrand and Willoughby canyons, respectively (Fig. 3D). Both flat areas are bounded by N070°E striking normal faults which are transverse to the general slope (Fig. 5C). In the Willoughby valley, the cross sections only reveal a small 10 m-deep V-shaped thalweg (Fig. 3D). However, the valley seafloor is characterized by a low reflectivity and any thalweg can be distinguished in the backscatter signature (Fig. 5D). To the North, the southeast flank of the Medusa mount is drained by several short canyons (up to ~ 20 km-long). Bedforms are visible at their mouth (small inset zoom on Fig. 5C). Across the Bertrand canyon, no large and infilled valley are found along the fault, and the thalweg shows a stronger reflectivity (Fig. 5D).
4) **Steepest slopes.** At 3000 mbsl, the canyons overspill the fault scarps, sharply turn clockwise at 90° and follow the general slope (Fig. 5C). Both profiles show spectacular knickpoints at these transitions and a convex-up and rough trend (Fig. 3D) with a high reflectivity (Fig. 5D). Both thalwegs broaden, and their cross-sections outline a rough bathymetry, departing from classical V- or U-shape (Fig. 3D).
5) **Canyon Mouths.** The distal portion of both canyons is characterized by a gently decreasing slope respectively towards the Desirade valley and the Falmouth Half Graben (Figs. 3D and 5C). Across Willoughby mouth, the shape is slightly mounded (blue profile n°12 on fig. 3D) and the reflectivity is high (Fig. 5D). Across Bertrand mouth, no mound is visible (orange profile n°10 on fig. 3D), however, the reflectivity is medium and higher than on the surrounding Desirade Valley seafloor (Fig. 5D).

4.2.3. Eastern boundary morphology of the forearc basins

The deep forearc basins are bordered by the steep slopes of the arc basement to the southwest and by the 2 to 13° gentle slopes of the accretionary wedge (Fig. 1C and 3A) to the northeast. Northeast of the Falmouth half-graben, where the slopes of the accretionary wedge are the steepest, in front of the Barracua ridge (red dashed line, Figure 3B, Laigle et al., 2103; Bénâtre, 2018) a horse-shoe headscarp can be distinguished in the bathymetry. It is associated to a ~23 km long and 12 km wide fan (Fig. 7A) which has a clear signature in the backscatter (medium heterogeneous, Figure 3) compare to the surrounding seafloor (low to very low heterogeneous). This fan extends far downslope and widen toward the basin to reach (Figs. 7B and 7C). The SB profile CAS-156 crosses the fan and shows that top transparent layers (Fig. 7D) overlay and seem to erode well-stratified reflectors. Those well-stratified reflectors onlap massive chaotic units that may formed by partly buried blocks. The headscarp is surrounded by very highly reflective zones which are 200-300 m-high mounds (Figs. 7B and 7C), that are likely mud volcanoes. We identified other slope failures in the area around the Meduse Basin (see Appendix C).

4.3. The "Channelized area" offshore Guadeloupe to St. Lucia

In the Channelized area, the islands and submarine guyots either belong to the outer arc (Grande Terre, Marie Galante and Dar Bien Phu-DBP and Amerique banks) or to the inner volcanic arc (Basse Terre, Dominica, Martinique and St Lucia; Fig. 8A). The water divide (Blue line on Fig. 8A) runs in between islands (From north to south: along the Saintes plateau, west and south of Marie-Galante, east of Dominica, along the western border of the DBP and Amerique bank, between the Martinique southern coast and the Sainte-Lucia northern coast). Between Guadeloupe and Martinique, the seafloor was gently tilted southward by 1.3° by normal faulting along the Desirade fault whereas it dips slightly (by 1°) to the northeast, northeast of St Lucia. As a result, the mid-slope of South and North Kalanina basins (4670 and 4720 mbsl, respectively), and the deepest (5170 mbsl) forearc Martinique basins, collect most of the sediments coming from the arc and forearc slopes through an important network of gullies and more or less developed canyons. The longest and deeper canyon of the area is the St Lucia canyon, which drains the slopes of the Sainte-Lucia islands. West of La Desirade, the Karukera spur is limited to the east by an up to 4000 m-high step cliff, which is incised by numerous short and straight canyons confined in the slope, and which all converge downslope towards the 5200 mbsl Karukera basin (Fig. 8A). A 1200 m-

high, NNW-SSE striking Arawak ridge separates the Karukera and Martinique basins. To the east, the counterslopes of the accretionary prism are the steepest east of Martinique basin, where a dense network of small gullies is developing. A 1000 m-high round-shape seamount (Hellene) limits the Martinique basin system to the south (Fig. 8A).

4.3.1. Eastern Martinique area

To the east, the Martinique island is surrounded by a large carbonate platform. It widens northwards and extends up to 10 km from the coasts, north of the islands (Fig. 9A). Several passes crosscut the fringing reef barriers, some were developed at the mouth of onshore tributaries. Beyond the carbonate shelf break, the insular slope extends over 85 km towards the forearc basins (Figs. 9A and 10). The sedimentary cover, which has a homogeneous reflective facies with a decreasing amplitude downslope (Fig. 8B), is imaged by seismic data (profile Agua 68, Fig. 10). It is made of three piled up units. Unit 1, the youngest, is made of high reflective continuous nearly parallel reflectors (blue on Fig. 10). Unit 2 is characterized by discontinuous and slightly hummocky reflectors (black). Finally, Unit 3, the deepest, is transparent with some discontinuous reflectors (green).

Six main canyons incise the most recent Unit 1: Caravelle, Robert, Vauclin, Paquemar, Hardy and Toiroux canyons which are 103, 78, 43, 21, 12 and 11 km-long respectively (Fig. 9A and 10). Their head settled on the carbonate shelf break which is 70-80 m deep at this location and they flow until fading out on the arc slope along a major W-E direction. Their walls underwent many landslides. Between the canyons, the seafloor is characterized by several sets of bedforms (Fig. 9A).

Canyons courses and profiles

The canyon heads have different shapes, in map view: triangular (Caravelle, Robert and Vauclin), amphitheater (Paquemar and Hardy) and an intermediate shape (Toiroux) (Fig. 9A). The morphology of the canyons is presented through longitudinal and cross-sectional profiles along the six canyons (Fig. 9B). All canyons main tributaries show a concave-up shape longitudinal profile and are connected to several secondary canyons originating from the carbonate shelf. They are deeply incised (up to 400 m-deep), narrow (~ 3 km-wide) and with a V-shape profiles. Their steep walls (~ 15°) are affected by numerous landslides, sometimes overhung by small tributaries with head confined in the slope. The Caravelle canyon has a second major tributary (Amerique canyon) that drains several well-defined slightly incised

(up to 150 m) gullies (Fig. 9C, profile e1) originating from the Amerique Bank. The Amerique canyon is different from other canyons with a convex-up longitudinal profile (Fig. 9C). All the canyons show a highly reflective facies, excepted two tributaries of the Caravelle canyon displaying medium reflectivity (Fig. 8B).

In the lower part where the slope flattens, the canyons resemble more to channels. They show a U-shaped and become less and less incised and finally fade out (Fig. 9A). At the difference, the Caravelle, Robert and Vauclin canyons have a very distinct and longer channelized section along the flat area, the Toiroux, Hardy and Paquemar canyons are shorter and rapidly fade out at the slope break (Fig. 9A), where a clear transition exists in the backscatter (from medium to low reflective; Fig. 8B). Downstream of the southern canyons, several discontinuous paleochannels can be distinguished (Fig. 9A). The Caravelle canyon widens and is up to 10 km-large at the slope break (cross-section a3 on Fig. 9B). Beyond 2000 mbsl the Caravelle canyon is very straight and shows an up to 4.5-km large U-shape with gentle sloping side walls dips (~ 5°) over a length of 40 km (Figs. 9A and 9B). The canyon fades out on the slope at 3500 mbsl. The Robert canyon evolves from a V to a U-shape, beyond the slope break (around 1500 mbsl) when the incision decreases (Fig. 9B, profiles b3 and b4). It veers from a N60° E to a N130° at 1000 mbsl and then veers back to a N60° direction just below 2000 mbsl. At this depth, a structure of medium heterogeneous reflectivity is identified numbered 1 on Figure 9A (Fig. 8B, Appendix D and more detailed description bellow in the section "Bedforms"). On the backscatter of Figure 8B, the Robert canyon is more reflective than the surrounding sedimentary cover. Beyond the 2000 mbsl kink, however, the width of the canyon decreases with the reflectivity. The backscatter on Figure 8B also reveals a small E-W more reflective furrow, in the prolongation of the Vauclin canyon, which, there, connects with the Robert system.

Slope failures

Several slope failures can be identified on the canyons walls (White lines on Fig. 9A). The largest portion of the Caravelle canyon (around 1800 mbsl) is bounded by walls, arched-shaped by numerous scars. The scars cannot be distinguished in the backscatter (Fig. 8B). Downstream at 2500 mbsl, a large slope failure with cuts across the northern wall of the canyon (Fig. 9A). It is clearly visible in the backscatter, underlined by high reflectivity (Fig. 8B). Downslope of those scars, the canyon is characterized by a rough morphology (Fig. 9A) with irregularities along the bathymetric profile (Fig. 9B), a higher and heterogeneous reflectivity compared to the surroundings (Fig. 8B) and a discontinuous seismic facies

(Fig. 10). A furrow is distinguished on top of the rough morphology around 1800 mbsl, with a more reflective pattern in the backscatter (Figs. 8B and 9A). This furrow is not identified downslope the landslide scar at 2500 mbsl until it reappears downstream with a clear trace in the bathymetry but not in the backscatter (Fig. 8B). We observed numerous slope failures along the bounding wall of other canyons, mainly upstream.

Sediment failures also affect the free slope. Between the Caravelle and Robert canyons, and from 1000 to 2600 mbsl, we observe a 2 km-wavelength alternation of linear and discontinuous 25 m-high crests and troughs over 20 km, on a 3° slope. These are confined in a horse-shoe shaped structure, bounded by up to 400 m-high scarps (structure numbered 2 on the Fig. 9A and section AA' on Appendix D). The upper part infill of the horse-shoe is imaged by the Agua68 profile, and shows parallel reflectors (Fig. 10). This structure has no signature on the backscatter (Fig. 8B). Upslope, several slope-perpendicular striking east-facing scarps disrupt the seafloor between 1000 and 1500 mbsl.

Bedforms

A remarkable 2.4 km-wavelength bedforms set extends downstream both at the mouth of the Vauclin canyon and beyond the 2000 mbsl kink along the Robert canyon (Fig. 9A). It dwells over a distance of 45 km, on a 1.7° dipping slope. Their height decreases downwards from 50 m to 20 m (zone numbered 1 on Fig. 9A and section BB' on Appendix D). They are neither spread on the entire slope nor confined in a structure. They have a clear signature in the backscatter, medium reflective stripes with increasing length away from the canyon kink (Fig. 8B). The lower part of these bedforms set has a low heterogeneous reflectivity superimposed by medium reflective structures (Fig. 8B).

Similar features are visible at the mouth of the Robert canyon (3000 - 3500 mbsl) on a lower slope gradient (~ 0,9°) (zone numbered 3 on Fig. 9A and section CC' on Appendix D). They have a ~ 500 m wavelength and show a clear signature in the reflectivity (Fig. 8B). They compose a fan-shaped zone of very low heterogeneous facies disrupted by low reflective arched structures.

Connection with onshore drainage system

Nine main rivers drain the higher reliefs of the islands (Fig. 9A), seven (Lorrain, Capot, Grande rivière, Galion, Carbet, Monsieur and Lézarde) in the north, flowing from the main quaternary volcanic complexes of Morne-Piton and Mount-Pelée, and two (Salée and Pilote)

in the south. All but three (Capot, Lorrain and Galion) flow towards the western part of the arc.

The main rivers of Lorain and Capot, to the north, flow on the 40 to 70 m deep platform, which is 9 km large at this place (Fig. 9A). It may connect to the Marigot submarine canyon, which flows toward the western part of the arc. However, no channel connecting the river to the canyon can be distinguished neither in the bathymetry nor in the seismic profile available in this area (Leclerc et al. 2015). Only submerged paleo-passes, probably disrupting an old drowned reef barrier, can be identified near the shelf break. The connection with the Caravelle canyon is even less straightforward but we distinguished very smooth, slightly E-W oriented depressions, that could be paleo-channels on the platform in the high-resolution bathymetry (Fig. 9A).

The sediments carried by the main Galion river may move into the Robert canyon trough passes within the double reef barrier (Fig. 9A). Beyond the reef, no paleochannel can be identified on the surface of the deeper platform. To the South-East of the island, the drainage systems are smaller and no large permanent river exists (Fig. 9A). Several passes disrupt the reef barrier in front of the main gullies. Several paleochannels were identified downstream of the main passes and upstream of the main courses of Vauclin, Paquemar and Hardy canyons. All paleochannels we identified show a smooth morphology.

4.3.2. St. Lucia canyon and southern canyon

South of Martinique, the arc slope is gentle, slightly convex and flanked by the Barbados accretionary prism and the Hellene Mount reliefs to the east (Figs. 8A and 9A). It forms a N40°E-striking gutter in the middle of which flows the St. Lucia canyon. The canyon originates from the western slopes of the St. Lucia island. Without any high-resolution data of the head of the canyon, it is impossible to know whether it connects or not to the island shelf break and how it linked or not to the main channels flowing onshore. The canyon streams on the slope of the arc, towards the Martinique basin, along a mean N40°E direction. It veers to a more N-S direction, at 3150 mbsl, west of the Hellene mount (Figs. 8A and 9A). Where high-resolution bathymetric data are available, we identified three distinct segments (S1 to S3 on Fig. 9A). The meandering S1 segment extends between 1800 m and 2200 mbsl. This segment is characterized by an up to 1.5 km-wide and up to 250 m-deep, V-shape thalweg (profiles f1 and f2 Fig. 9B) which is flanked by terraces in the inner loops (blue arrows, Fig. 9B). The second segment thalweg, between 2200 and 3000 mbsl is also V-shaped, deeply incised (~

420 m) and bounded by up to 4 km-wide terraces. The edges of the terraces (blue arrows on the profiles f3 and f4, Fig. 9B) and the abandoned external bounding cliffs are over-incised and form paleo-meanders, having the same sinuosity than the ones of segment S1. The St Lucia thalweg is straighter in the lower part of the S2 segment (Fig. 9A). There, it strikes N35°E and is bounded by two steep 40 m-high cliffs. Segment S3 is striking N05°E. Its incision decreases downwards to reach less that 20 m before it fades out on the slope at 3500 mbsl (profile f7 on Fig. 9B). Along this portion, we can identify bedforms on both sides of the canyon in the backscatter but the bathymetry resolution prevents to determine their characteristics (Fig. 8B). They are perpendicular to the channel direction and more pronounced on the NW of the channel with their height and their wavelength which seems to decrease downslope. In addition to the St. Lucia canyon, the smooth relief that goes up to 1700 m-depth and is about 70 km-large (Fig. 1B), which separated the Tobago and Martinique basins, is cross-cut by a paleo-canyon (Fig. 8A).

4.3.3. Forearc slope from Amerique Bank to Dominica Island

North of Martinique, from the Amerique bank to the Dominica island, the arc slope dips gently by 2° and increases abruptly to reach 7°, where a steep scarp bounds the Martinique Basin to the east, in the prolongation of the Karukera scarp (Fig. 11A). The gentle part of the slope is crosscut by numerous active normal faults that are up to 60 km long and mainly N90°E and N130°E-striking (Fig. 11A). The faults displace the most recent sedimentary layers down to the seafloor. Their scarps, up to 400 m-high, partly control the course of the main canyons of the area (Kalanina, DBP1, DBP2, Bruce Castle canyons -and its tributary, Melville Hall canyon- 58 km, 25, 19 and 105 km-long, respectively; Fig. 11A). Downslope, the faults bound the N120°E-striking Kalanina north and south graben (Fig. 11A).

The Bruce Castle and Melville Hall canyons, which are respectively up to 300 and 220 m-deep (Fig. 8C), probably originate from the shelf of the Dominica islands. However, no high-resolution data exists in this area to confirm this (Fig. 11A), nor their link with the largest rivers flowing from the highest volcanic reliefs (Morne Diablotin and Morne Trois Pitons, 1421m and 1394m high, respectively). The up to 190 m-deep DBP1, up to 190 m-deep DBP2 and up to 200 m-deep Kalanina canyons originate from the round-shaped Dien Bien Phu and Amerique banks (respectively 95 km^2 and 130 km^2). The banks are 70 to 80 m-deep and are thus emerged during sea-level low-stands (Fig. 11A).

The canyon heads are very different from the ones we observed in Martinique. They are composed by downward merging 40 to 100 m-deep rills or gullies (see map of Fig. 11A and cross-sectional profile of Fig. 8C). Almost all canyons and gullies are straight and flow in a N90°E direction, along the normal fault traces. The central part of the Bruce Castel canyon and the gullies upstream Kalanina and DPB1 canyons however strike N70°E and N30°E, respectively (Fig. 11A). In locations where the Kalanina canyon flows across the scarp of the N120°E fault set, we observe a small knickpoint along the canyon longitudinal profile (Fig. 11B, see appendix E).

Several slope failures were identified along the canyon walls (Fig. 11A). Their scars have a classical "spoon" shape, whereas others have a more complex morphology, with a wider and more elongated following the direction of the main fault. The largest one (10 km long) lies on the southern wall of the Kalanina canyon (Fig. 11A). At some places, the slumped material remains within the canyon, forming dams marked by knickpoints just downstream of the scars (see for example knp1 and knp2 along the Kalanina canyon on Fig. 11B).

The longest canyon of Bruce Castle flows into the Martinique basin, while the others fade out on the slope before reaching the Kalanina mid-slope and Martinique basin (Fig. 8A and 11A). It is deeply incised (~ 500 m) with a V-shape cross-section (Fig. 8C). It is characterized by a clear signature in the backscatter (Fig. 8B). Its thalweg is very reflective along the steepest slope of the scarp bounding the Martinique basin to the west. At this location, a knickpoint with a huge, up to 1200 m-high, face marks the longitudinal profile of the canyon (Fig. 8C).

4.3.4. Arawak canyon

The longest canyon of the Channelized area is the Arawak canyon (140 km-long) which drained an area with a complex morphology (Figs. 8A and 12). This area consists of a volcanic active island (Basse-Terre), two carbonated islands (Grande-Terre and Marie-Galante) and a shallow carbonated bank (Colombie bank, 40 m-deep). The largest carbonate platform (up to 15 km) is the Banc des Vaisseaux to the south-east of Grande-Terre and La Desirade (Fig. 12). Two other small carbonate islands exist (Petite-Terre islands) on the banc des Vaisseaux.

To the east, the area is limited by the eastern border of the Karukera spur. Two main valleys have developed in the area, the straight and narrow N130°E Marie-Galante valley between Grande-Terre and Marie-Galante and the large, amphitheater-shaped, Petite Terre

valley between Marie-Galante and the Karukera spur (Fig. 12). Both valleys converge downstream to merge in the Arawak valley. The backscatter data displays a very heterogeneous reflectivity (Fig. 8B). The Karukera spur and the slopes south of the Banc des Vaisseaux and north of Marie-Galante are highly reflective, whereas the valley have a low to medium reflectivity (Fig. 8B).

The Lézarde and Moustique rivers drain the main up to 1300 m-high reliefs (Matéliane, Morne-Moustique) that delimit the recent volcanic complex of Basse-Terre to the north (Fig. 13A). Both rivers flow in the *Petit-Cul de sac Marin* bay and may connect to the deep Marie-Galante valley through the main pass we numbered 1 on Figure 13A. The Petite Goyave river drains the same reliefs and flows into the Sainte-Marie bay and may connect to the deep offshore domain by the pass we numbered 2 on Figure 13A. To the south, an up to 3 km-wide, 10 m-deep, narrow carbonate platform separates the onshore of offshore domain and is disrupted by small passes. Moreover, no canyons are presently developing at the mouth of the rivers. The SB profile Gwad-Gua1 shows that an up to 45 m-thick transparent sedimentary unit has pounded at this place, within a depression at the base of an E-W normal fault scarp that prolongs westward the Morne-Piton fault (Fig. 14). By considering a velocity of 1500 ms^{-1} in the water and uppermost sediments, we calculated that the fault offsets the older unit by about ~ 40 m and the younger transparent unit by 2 meters at the seafloor. Although not distinguishable at the base of the scarp, the dark reflectors composing the older sedimentary unit (orange surface on Fig. 14), seems to be continuous on the fault hanging-wall. Therefore, it seems unlikely that it was carved by a paleo-canyon. However, we cannot exclude that a very small rill or gully was flowing at the base of the scarp.

While no paleo-channel was identified on the banc des Vaisseaux, three short paleo-channels were observed on the shelf break, west of Marie-Galante (red arrows on Fig. 13A). A submarine cone, which seems incised by a paleo-channel, can be distinguished in the bathymetry (though seismic data are needed to confirm this) at the mouth of a river (Fig. 13A).

Tributary drainage systems

The tributary drainage systems all converge downstream to supply the Arawak canyon. Along high-reflective steep (8-10° slopes) and rough cliffs (Fig. 8B), the heads of the canyons (some originating of the shelf break: a1, a2, c, e1 and e2 canyons from Banc des Vaisseaux, and 1a, 1b, 2, 5a, 5b and 10 canyons from Marie-Galante platform; others confined in the

slope: b, d and f and 3, 4, 6, 7, 8 and 9 canyons, Fig. 13A) are up to 12.5 km-long, up to 2 km-wide and deeply incised (up to 200 m) attesting for long-lived structures. The SB profile CAS-139 shows that the canyons incise into a transparent acoustic layer (Fig. 13B).

Eastwards, the lower reflective gentle slopes (2.5 to 5°) are drained by rills and gullies (Figs. 13A and 13C). They also are pounded by a thin sedimentary unit made of horizontal laminated reflectors as revealed by the profile CAS-139 (Fig. 13B). Southwest of Grande-Terre, a large network of very slightly incised (10 m), sub-parallel rills of similar short length are confined at the shelf-edge between 250 and 450 mbsl (Fig. 13A). Although very discrete in the bathymetric data, all rills have a sharp signature in the backscatter, being much more reflective than the surrounding slopes (Fig. 13C).

Three main up to 100 m-deep and 900 m-wide gullies lie at the mouth of the main reef passes, east of Basse-Terre (Fig. 13A). They cut across a cluster of up to 10 m-high and 250 m-large, very reflective blocks (Fig. 13A and 13C), which signature is also very characteristic on the profile Gwad-Gua1, inducing bright spots (hyperbolae) (Fig. 14). No submarine scar was observed around the blocks, but we can notice that the carbonate shelf has an arcuate shape and that the reef barrier is disrupted at this place (at the mouth of the Petit-Cul-de Sac; Fig. 13A). Between the blocky zone and the Colombie tributary, several paleochannels can be identified (Fig. 13A). Northwest of Marie Galante, a significant tributary (Colombie) with four arcuate-shaped canyon heads upslope is confined on the slope with no connection to an active channelized system (Fig. 13A).

All tributaries converge towards and flow into the Arawak canyon (named Marie-Galante valley at this location). The blocky zone is elongated downstream within the canyon (Fig. 13A), suggesting that the landslide deposit was confined within the canyon (valley). In its upper part and over 85 km between Basse-Terre and the western slopes of the Marie-Galante island, the Arawak canyon has a concave-up longitudinal profile (Fig. 8C). In this part, the canyon strikes N100°E, shows a wide U-shape (orange profile numbered 2 on Fig. 8C) and it is characterized by a medium to low reflectivity (Fig 8B). The canyon floor is covered by bedforms that have concave arcuate crests (crescent-shaped) perpendicular to the main channel axis (Fig. 13D). Bedforms having the same morphology can also be identified in the largest canyon originating from the Banc des Vaisseaux (e1 on Fig. 13A).

Downstream, the Arawak canyon flows along the Morne-Piton fault scarp over 10 km (Fig. 8A). At this location, a small depression was dug at the base of the scarp (Fig. 8C). When passing the scarp to the east, the canyon veers to a N130°E direction and flows southwards

over 55 km before merging with the Bruce canyon (Figs. 8A and 11A). Along this portion, it is narrow (Fig. 8A) and it has a convex-up profile (Fig. 8C) and very reflective (Fig. 8B).

4.3.5. Martinique basin

The Bruce Castel canyon plunges into the Martinique forearc basin which is 75 km-long, 30 km-wide and 5175 m-deep elongated in a NNW-SSE direction (Fig. 15). It is bounded by the steep straight scarp of the arc basement to the southwest and by the gentler, smooth 2° dipping slopes of the accretionary prism to the northeast. A large sediment lobe (Section AB on Fig. 15) has developed at the mouth of the Bruce Castle canyon. We identified small paleo-channels in the prolongation of the Kalanina and DBP canyons (a, b and c on Fig. 15) and East of the South and North Kalanina basins (d, and e in Fig. 15), which indicates that connections may have existed in the past. A meandering paleo-channel (f on Fig. 15), which has deeply incised the basement scarp, used to flow in the Martinique Basin. It is not active anymore and its head has been sharply disrupted and disconnected (probably from the DPB1 canyon) by the N130° normal faults which compose the South and North Kalanina graben. Several short and straight canyons drain the steep Karukera scarp east of the basin (Fig. 15).

To the north-east, a spectacular network of slightly incised (up to 35 m-deep) gullies are clearly visible in the bathymetry. The gullies are confined in a large wide horseshoe-shaped structure bounded by up to 500 m high walls (see bathymetric profile CD on Fig. 15). The origin of such a structure is unknown. To the south (zone 1 on Fig. 15), we find shorter and straighter gullies, up to 11.5 km long, which vanish at the toe of the slope (around 5100 msbl). To the north (zone 2 on Fig. 15), gullies are twice longer and dendritic. They have developed over a distance of ~50 km, due to regressive erosion on the slope of the accretionary wedge. They incise the basin floor and the sediment lobe at the mouth of the Bruce Castle canyon. All around the Martinique Basin, several other small horse shoe-shaped steep scarps exist, suggesting that landslides occurred in the past (Fig. 15). The sedimentary cover in this part of the forearc and prism is highly deformed by N-S-striking thrusts (Bénâtre, 2018). Several rills incise the anticline structures and flow in the piggy back basins (Fig. 15).

5. Discussion

5.1. Transfer and sediment input along the slopes and forearc basins

5.1.1. Onshore drainage and carbonate platforms

The Lesser Antilles arc is composed of active volcanic islands, which are incised by several large rivers able to erode and transport a large amount of sediment. Rad et al. (2013) demonstrated that the mechanical erosion rate of the active volcanic complex in the Lesser Antilles is important, up to 4000 t/km^2/yr, and one of the largest worldwide. The estimated mechanical erosion of the older relief in Guadeloupe is lower (Rad et al., 2013), but still important compared to other rivers worldwide. In such conditions, the rivers draining the slopes may transport a large amount of sediments. The islands are surrounded by reefs and lagoons which may, however, retain a large part of those sediments, thus limiting the sediment supply into the heads of the forearc canyons and downslope in the mid-slope and forearc basins.

In Martinique, only one permanent river (Galion river) flows towards the east but it drains much lower and older reliefs than those of the active Mount Pelée volcanic complex (Fig. 9A). Nowadays at high-stand, the double reef barrier situated at this location may act as a dam retaining most of the sediment loaded by this river. A large ~10 m-thick Holocene sedimentary unit has been imaged with seismic data (Leclerc et al., 2015) in the deep and large lagoons and bays (Galion, Robert) in between the coast and the reef barriers (Fig. 9A). It may transfer to the deep canyons of Caravelle and Robert at low-stand, although no clear incision can be seen on the platform (Fig. 9A). The incisions identified on carbonate platform (Table 3 and Fig. 9A) are probably inactive, buried and overtopped by the Holocene reef. They have likely connected the terrestrial and offshore system in the past, probably during the last glacial period, when the sea level was lower. In Guadeloupe, however, several main rivers flow toward the east and may bring an important fraction of siliciclastic material in the deep offshore system (Fig. 13A). The reef platform is shallow, narrow and large passes have developed at the mouth of the main rivers draining the highest reliefs of Basse-Terre (Fig. 13A); maybe allowing for easier connection, even in periods of sea-level high-stands. The Capesterre and Perou rivers drain the young volcanic reliefs of Grande-Découverte and surprisingly no marine canyon exists at the mouth of the rivers (Fig. 13A), as well as at the mouth of the Goyave river (Fig. 12).

Nowadays, an important seiche, triggered either by the tidal current or by the waves that are even more energetic along the eastern coasts (Cambers, 2005; Woodworth, 2017), occurs almost continuously on the carbonate platform of the Lesser Antilles (with maximum amplitude of 20 cm measured in large bay Pointe-à-Pitre in Guadeloupe and Le Robert in Martinique; Woodworth, 2017). This helps to keep the finer fraction of sediment originating from the platform in suspension. During hurricanes, the waves are even much larger, and a lot of fine-grained sediments can be put in suspension or transported within the lagoon or near tidal passes. Sedimentary structures evidencing transport on the platform have been documented and associated to the David and Allen Category 4 hurricanes in 1979 and 1980, respectively (Durand et al., 1998). More recently, the satellite images taken after the hurricane Irma in Florida reveal that a large amount of sediment was suspended in the surrounding lagoon and retained within the reef barriers (https://www.nesdis.noaa.gov/content/viirs-sees-irma-churned-sediments-around-florida-bahamas). After this hurricane, large plumes of fine suspended sediments originating from the platform were exported several to tens of kilometres away from the coast of the Antigua-Barbuda platform (https://earthobservatory.nasa.gov/images/90952/hurricane-irma-turns-caribbean-islands-brown). Mulder et al. (2017) propose that these fine-grained suspended sediments can be further flushed from the lagoons by strong currents at the tidal passes.

5.1.2. Shelf-edge offshore southeastern Guadeloupe

We described several structures at the carbonate platform-edge in the Channelized area, which were not observed along the Rough area where the slopes are probably too steep. At the Basse-Terre shelf-edge, we identified an up to 45 m-thick transparent sedimentary wedge (Fig. 14). It was deposited upon an older unit, which is composed of more-reflective sub-parallel reflectors, at the edge of the carbonate platform, on the hanging-wall of the Morne-Piton normal fault. By comparison with the sedimentological observations made along the edge of the Bahamas platform (Mulder et al., 2017; Fauquembergue et al., 2018), we think that this transparent wedge could be a Holocene deposit, made of fine-grained sediment of the shelf, though more data (i.e. sediment cores) would be needed to confirm this. Those deposits were inferred to be mainly the result of the export and downslope transport of sediments by density cascading during episodes of winter cold fronts (Wilson and Roberts, 1995, Mulder et al., 2017; Fauquembergue et al., 2018). On the large Bahamian carbonate platforms, Wilson and Roberts (1995) concluded the density cascading generated by cold fronts throughout all the platform is a major process allowing off bank export of fine-grained remobilized

sediments. Some cold fronts reach the Lesser Antilles islands but less frequently than in Bahamas (Dimego et al., 1976). Without any further information on water stratification on, and within, the Lesser Antilles carbonate shelf, we cannot confirm the existence of such processes. However, Reid et al. (1996) demonstrated that fine-grained suspended sediments are expulsed from the shallow platform, mainly westwards by the contribution of strong currents (Johns et al., 2002). The older unit was probably deposited during the last glacial period between the MIS5 and MIS2. Since the last glacial maximum which is 20 ky in the Caribbean (Clark et al., 2009), it has been offset by ~ 40 m implying slip rate of 2 mm/yr on the Morne-Piton fault (Figs. 13A and 14). This is twice the slip rate determined based on a morphotectonic study of Quaternary marine terraces in Marie-Galante (Feuillet et al., 2004), but still very coherent. This reinforces our interpretation on the age of this wedge. This means that an up to 45 m thick layer of sediment has been deposited during the Holocene in this area implying a mean sedimentation rate of 150 cm/ky, five to ten time larger than those estimated by Reid et al. (1996) but of the same order of size than those estimated by Beck et al. (2012) in basins of the western part of the arc. We highlighted that no large canyon has incised the older unit below the transparent wedge which spread at the mouth of the Capesterre and Perou rivers (Figs. 13 and 14). It suggests that the erosive power in front of such river is weak, even at low-stand.

South of Grande-Terre, a dense set of rills and gullies developed at the base of the carbonate slope break between 350 and 450 mbsl (Fig. 13A). Such a set of small sub-parallel gullies have been documented along the slopes of the Bahamas margin up to the same depth (400 m) and interpreted as resulting from density cascading phenomenon with activity of plunging currents reaching the seafloor at 400 m water depth (Principaud et al., 2018). The gullies initiation is still not well understood. Lapuyade (2015) and Principaud (2015) proposed that fine-grained sediments exported from the platform can exceptionally concentrate and generate a low-density turbidity flow which may further incise the slope initiating the formation of rills. The sedimentary cone developed at the shelf-edge offshore the main river of Marie-Galante (Fig. 13A) suggests that sediment has accumulated at the insular shelf-edge rather than having transited in deeper areas. However, the paleo-channel seems imply that onland-offshore transfer may have occurred in the past.

5.1.3. Sediments through the canyons

The thalwegs of the canyons connected to the carbonate platforms are more reflective than the adjacent seafloor, implying either coarser deposits or the outcrop of the basement. It suggests that sediment is carried through these canyons. Other observations support this interpretation: 1) the morphology of the canyon upper parts is marked by V-shaped cross sections and concave-up longitudinal profiles evolving to U-shaped cross sections downstream, which indicate erosive processes followed by depositional processes; 2) the reflectivity decreases downslope of the thalweg, likely linked to the decrease of the grain-size and accumulation of deposits, which suggests a dynamical sorting along the thalweg; 3) sediment lobes are identified at the mouth of some canyons in bathymetry and/or reflectivity, implying sediment accumulation; and finally, 4) several patches of bedforms (some crescent-shaped) lie inside the canyons or at the mouth of the channels (Fig. 16). Their wavelengths and their heights are of the same order of size than others observed worldwide, either inside (Wynn and Stow, 2002; Paull et al., 2010; Babonneau et al. 2013; Normandeau et al., 2014) or outside the submarine canyons (Rebesco et al., 2009; Normandeau et al., 2014). Crescent-shaped bedforms have been interpreted as the result of gravity flows (Paull et al., 2010). It thus appears that, at low and high-stand of sea-level, the canyons can be active during exceptional events such as storms, density cascading episodes, seismic event or slope failures.

At sea-level high-stand, we previously highlighted that sediment can be exported from the carbonate platforms along their edge at shallow depths. Thus, it is likely that sediments remobilized from the platform during hurricanes or density cascading events accumulate in the canyon heads (Puig et al., 2004). Offshore Martinique, the Caravelle canyon is characterized by medium reflectivity, whereas farthest south canyons have a high reflective thalweg. All the canyons but the Caravelle one are in front of reef barrier passes (Fig. 9A). The difference in reflectivity can be explained either by finer-grained sediments carried through the Caravelle canyon or by the presence of a thicker hemipelagic sediment drape and thus a reduced turbiditic activity. In addition to sediments originating from the carbonate platform, the canyons can also carry out the sediments which are remobilized when the canyon's walls collapse. The rough morphology at the base of theses scarps suggest that part of the remobilized sediments settled inside the canyons as a MTD. Those MTD filled the canyon and act as dams further retaining most of the sediments coming from upstream. The existence of a furrow in the Caravelle canyon (Fig. 9A) shows that those MTD can be further eroded, however, enabling the sediments to be transported downstream again.

The longitudinal profiles of the canyon are disrupted by several knickpoints of different origins: i) tectonic when crossing active normal fault scarps, ii) sedimentary when the canyon is trying to incise a dam induced by a previous mass transport deposit, or iii) lithologic when the canyon flows along a less erodible geological unit (basement). For instance, it is likely that the Mesozoic basement outcrops along the lower part of the Bruce Castle canyon where the reflectivity is very high, the scarp being in the prolongation of the Karukera spur. This attests that the sedimentary transfers are not enough efficient to erode the cliff inside the canyon either because it grows continuously due to tectonics, because the wall collapses are recurrent or because it crosscuts less erodable and harder geological units. Both situations prevent the canyon from reaching an equilibrium profile.

The mapping of the systems allows the identification of the nature of the remobilized sediment: purely carbonated from carbonate platform belonging to the outer arc; mixed siliciclastic-carbonate from shallow platform surrounding inner arc islands; and siliciclastic from the old Mesozoic basement which out crop on the Desirade island, likely along the Desirade fault scarp and on the high reflective Meduse mount (Fig. 3B). Thus, those shallow platform sediments can reach the deeper mid-slope or forearc basin only if they are further remobilized in high-energy currents. Slope failures may occur locally when too much sediment has accumulated, the slope has steepened too much or because they are destabilized over a larger scale by a strong earthquake, canyon flushing (Canals et al., 2006; Piper and Normark, 2009; Mountjoy et al., 2014, 2018).

5.1.4. Sedimentation in the basins

In the Rough area, several basins are completely disconnected from the shallow carbonate shelf and originate from slope that are deeper than 500 mbsl (Table 3, in red on Fig. 16). They are thus too deep to be affected by the storm waves, even at sea-level low stand. Along such slopes, the sedimentation rate is low (~ 3 cm/ky, Reid et al., 1996) and there is no sediment input from the terrestrial system. It is thus unlikely that local slope failures due to sediment load occur frequently. The more likely ways to remobilize sediment along these may be widespread landslides and turbidity currents triggered by an earthquake shaking. We identified hummocky deposit around the shallow Falmouth and Bertrand banks attesting for failure of their slope (Fig. 5C). This may have generated high-energy currents able to propagate over long distance and to feed the adjacent Falmouth valley but also the deeper forearc basins at the mouth, Desirade Valley, Desirade half graben (and maybe Desirade

Basin) and Falmouth half graben. The Falmouth spur is crossed by two main canyons which have a similar pattern. However, the lobes at their mouth are characterized by different reflectivity (Fig. 3), which could imply different grain-size, coarser at the Willoughby mouth. This suggest that the dynamical sorting of the sediments is less efficient in the Willoughby canyon. The Bertrand canyon has a high reflectivity all along its course which could imply that the canyon carry out the sediment from the head to the mouth all at once, whereas the Willoughby canyon is not distinguished in the reflective map throughout the Willoughby valley. These observations allow us to conclude that the Willoughby valley is a current depocenter, and not a by-pass area, fed by sediment from the Falmouth valley and Meduse mount, and thus that it feeds the Falmouth Half Graben. Besides the slope instabilities, basins figured in red on Figure 16 are fed by canyons connected to shallow platforms, which are emerged at low sea level (Table 3, in yellow on Fig. 16). This may imply additional trigger as hurricanes to the turbidity currents which reached these basins. All deep forearc basins also receive sediments from the slopes of the accretionary wedge, within which very different types of sediments (composition and textures) can be reworked (Stéphan et al., 1990; Beck et al., 1990; Capet et al., 1990), this concerns Paleocene to Pleistocene deposits.

In the Channelized area, only the Bruce Castle canyon on which merge the Arawak and Melville Hall canyons flows into the Martinique basin (Fig. 16). Thus, its sedimentary record may be different from that of the mid-slopes Kalanina basins which are not supplied by canyons (Table 3). The Martinique Basin may collect a mix of carbonate from the reefs and siliciclastic sediment from the Martinique, Dominica, Guadeloupe and maybe St Lucie volcanic islands. Slope failures along the insular slope and accretionary prims are probably the most important phenomena able to bring a huge quantity of sediment in the Martinique basin. To the east, the Martinique Basin is fed by a dense set of gullies that incise the foothill of the accretionary prism. Those gullies may be formed either because deep downslope currents exist in this area (as shown in New-Zealand; Micallef and Mountjoy, 2011) or because the slope is steepened by tectonic uplift in front of the Tiburon Ridge (Bénâtre, 2018). The second hypothesis is more likely, since no other similar sets of gullies were identified along the slopes of the accretionary wedge.

5.2. Origin of most important morpho-sedimentary structures

5.2.1. Slope failures

Rough and Channelized areas show traces of large slope collapses and landslides (Table 3 and Fig. 16) with different possible triggers depending on their depth. Our observations imply that slope failures occurred at different time-scales along the forearc, which can be outlined by the reflectivity. Most of the scarps are not distinguished on the adjacent areas, suggesting that they are pounded by hemipelagic sediments, whereas some are characterized by higher reflectivity, implying most recent failure.

The landslide scars along the Falmouth basin eastern slope occurred on the foothill of the accretionary prism in an area where lie numerous very reflective rounded reliefs, that we inferred to be mud volcanoes (Fig. 7), similar to those documented south of Barbados islands by Deville et al., (2010). At this place, the wedge is deformed, and the slopes are over-steepened by the entering in subduction of the main Barracuda ridge (Bang et al., 2003; Laigle et al., 2013; Bénâtre, 2018). The over-steepening of slopes, coupled to an excess of pore pressure in an area where fluids or gas circulate may have favored landslides by decreasing the shear strength of the sediments down to a failure threshold (Pratson and Coakley, 1996; Maslin et al., 1998; Dugan and Flemings 2000). Such slopes are more prone to destabilization during earthquakes (Green and Uken, 2008; Stigall and Dugan, 2010).

In South of Guadeloupe, the MTD in the Arawak canyon head is characterized by blocks with a clear signature in the SB profile and lie over the dark sub-parallel unit probably deposited during the last glacial period (Fig. 13). They were thus probably deposited either during rapid rise of the sea level at the last interglacial glacial transition or during the Holocene. Thus, this event could be similar to the 14 ky-old mass deposit documented south east of Antigua by Trofimovs et al. (2010), which coincides with the last sea-level rise and inferred to have been triggered either by sea-level change or seismic shaking (Trofimovs et al., 2010). Indeed during such period, it is the main re-flooding window of the platform, allowing the initiation of the carbonate production (Jorry et al., 2010) and carbonate slopes are unstable, making the slope more prone to failure particularly when an earthquake occurs. Though a volcanic origin has also been proposed more recently (Trofimovs et al., 2013). The paleochannels identified in this area may have been buried by the landslide deposit. Indeed, the numerous slope failures impacted the evolution of the canyons. The change of direction in the course of Robert canyon could have been generated by an old landslide which could have

occurred on the interfluve between Vauclin and Robert canyons (Fig. 9). The bedforms at the kink of Robert canyon, seem to be a set of sediment waves of a spill over lobe generated by the flow stripping of the gravity currents carried by the Vauclin and Robert canyons downstream.

5.2.2. Canyons

The distinct morphological background of the Rough and Channelized areas could imply different origin of the canyons. In the channelized area, the forearc basement is covered by thick piles of sedimentary (profile Agua68; Fig. 10). By comparison with older seismic profiles (Bouysse and Guennoc (1983), the Units 1 and 2 (Fig. 10) were likely deposited after the mid-Miocene period, after the outer arc had ceased its volcanic activity. The acoustic signature of Unit 2 unit suggests that it could be made of more clastic sediments originating from the erosion of the high reliefs of the outer arc. Unit 1 is most likely made of carbonate layers piled up on the slope since the development of the carbonate platforms around and on top of abraded reliefs of the outer arc. The main canyons incise the most recent Unit 1, suggesting that they initiated together with the development of the carbonate platform. South of the Banc des Vaisseaux, the canyons are characterized by a low to medium reflective thalweg and very high reflective interfluves (Figs. 8 and 13), contrary to what has been described offshore Martinique. It suggests that these canyons may evolve into the volcanic basements. The Rough area is shaped by normal faults characterized by high cliffs. Most of the canyons formation and evolution might have been influenced by faulting.

Our observations indicate that canyons east of Martinique (Fig. 9A) and north of Marie-Galante and Colombia Bank (Fig. 13A) may have initiate and enlarge through retrogressive canyon failures as documented along active margin in Portugal (Lastras et al., 2008) or in Sicily (Iacono et al., 2011) or along other carbonate platforms in Australia (Puga-Bernabéu et al., 2011) and in Bahamas (Mulder et al., 2012; Tournadour et al., 2017). The existence of rills and a wedge of fine-grained sediment along the slopes of the Guadeloupe insular shelf suggests that downslope currents are also carving the sediment (Fig. 13A). Some of those rills have been captured by adjacent rills to form longer and more incised gullies. Those gullies may eventually evolve into a larger canyon. Such process which was proposed to explain the formation of canyons (Pratson and Coakley, 1996) was modelled in a sandbox by Lai et al. (2016) by releasing a continuous unconfined flow on an over-steepening slope. The resulting morphology of the simulated canyons resembles to those we identified in the channelized

area. This hypothesis of downslope erosion may explain the initiation of canyons which heads are connected to the insular shelf break or confined in slopes but along which deep currents are plunging (Micallef and Mountjoy, 2011).

It is likely that the two processes occur coevally (retrogressive upslope erosion and downslope erosion) to initiate and carve the canyons as suggested by Puga-Bernabéu et al. (2011). The later authors propose that the canyons they documented in Australia originate from a landslide, comparable to that we identified east of Martinique (structure numbered 3 on Fig. 9A), and then further grow by retrogressive upslope erosion. Once the canyon reaches the shelf break, its activity may be enhanced by the downslope transfer of sediments from the shelf or from the terrestrial systems.

5.3. Tectonic control of the drainage system

All the drainage system is controlled by the tectonics in the eastern part of the Lesser Antilles, may it be, at a local scale by individual faults, or at a regional scale by the entering of large ridges in the subduction, for example (Bouysse and Westercamp, 1990; Laigle et al., 2013; Bénâtre, 2018). Active tectonic controls the initiation and abandon of drainage systems, the course and the longitudinal profile of the canyons (convex-up shape in an uplifting context), the sediment inputs and transfers, the erosion and sedimentation rates (Greene et al., 2002; Micallef et al., 2014; Laursen and Normark 2002; Noda et al., 2008; Ratzov et al., 2012).

The Desirade fault scarp is the largest and steepest of the area (up to 4000 m-high) (Fig. 3A). The fault separates two areas where the drainage system is very different (the Rough and the Channelized area; Fig. 1C). Slip on this fault has tilted the whole area of the Karukera spur to the south, at a regional scale (Feuillet et al., 2002, De Min, 2014), and has influenced the sedimentation style in the area as well as the development, the course and the longitudinal profile of the main Arawak canyon. Indeed, it is noteworthy that this portion of the canyon strikes parallel to the N130° normal faults identified in this area, and thus, may suggest a structural control. To the south, the St. Lucia Ridge has contributed to deform the accretionary wedge and the forearc domain (Laigle et al., 2013). This may have influenced the development of the drainage system and the sediment transfer in this area (Figs. 9A and 16). Though high-resolution data are missing in the area, we have identified a folded paleo-canyon at the tip of the ridge (Fig. 16). The canyon probably used to connect the Tobago and Martinique basins. It is now inactive, and a wind-gap has developed in the middle of the

canyon. In its middle part, the St. Lucia canyon is meandering on a slope that has been probably flattened by uplift, in front of the ridge (Fig. 16). Well-formed terraces have developed in the canyon. Though we have no SB profiles to confirm this, those terraces may result from incision due to tectonic uplift as shown elsewhere along the Japanese active margin for example (Noda et al. 2008) rather than from landslides, as documented along canyons of the Bahamian carbonate platform by Tournadour et al. (2017). The uplift and tilting of the Karukera spur and of the forearc offshore St. Lucia control the slope and thus the drainage system at the scale of the arc, making all the main canyons flowing towards the Martinique basin (Figs. 8A and 16). On the northeastern border of the Martinique basin, the slope of the accretionary wedge is steepened by the entering of Tiburon ridge (Laigle et al., 2013) and a dense set of gullies flowing toward the arc has developed in this area (Fig. 15). The gullies are confined in a huge horseshoe structure whose origin is unknown, but may correspond to a very large landslide scar at the tip of the Tiburon ridge.

At a more local scale, the arc perpendicular normal faults cutting the seafloor of the eastern part of the arc (Feuillet et al., 2011) are controlling the main canyon courses and the formation of the mid-slope or deeper forearc basins (Fig. 16). Their scarps are steep slopes on which numerous canyons have developed. Some canyons cutting across the fault and knickpoints are developing at the intersection with the fault scarp along the longitudinal profile of the canyon. This may have influenced the behavior of the canyons, which tend to erode the seafloor at those places. Some canyons were beheaded by faults and are now inactive. Depressions and grabens lying at the base of the scarp or between antithetic faults store the sediments transported by the canyons. They may also behave as intermediate retention basins, in which sediments may be stored before being transported in deeper basins. As an example, the Willoughby valley may keep a part of the sediments supplied by adjacent slopes (Fig. 5C). Those sediments could be further remobilized during high-energy currents channelized in the narrow Willoughby canyon and deposited downslope in the Falmouth half graben. The Morne-Piton fault controls the course and the behavior the Arawak canyon (Fig. 12). North of the fault, the canyon is large, U-shape and low reflective, overall indicating that sediment accumulate there, on the subsiding hanging-wall of the fault (Figs. 12 and 13A). In opposition, once the canyon crosses the fault and flows on the uplifted foot-wall of the fault, it becomes narrow and more reflective attesting for incision of the sediment (Figs. 12 and 8).

As observed elsewhere large earthquakes on the subduction interface may induce local or regional slope failures, canyon flushing and high-energy currents able to erode the slope and

canyon upslope and to transport huge quantity of sediment downslope over several hundred kilometers. Smaller local crustal faults may also influence the sedimentation (Beck et al., 2012). We have observed this between Basse-Terre and Marie-Galante. A small depression is created at the base of the Morne-Piton fault scarp by faulting. This tends to retain the sediments coming from the shelf in front of the main Rivers that drain the active volcanic complex of Basse-Terre (Fig. 13A). At this place, the fault has offset the sediments of the last glacial period by 40 m (Fig. 14). The younger sediments composing the Holocene wedge were deposited at the base of the scarp and are offset by 2 m (with the hypothesis of a P-wave velocity of 1500 m Td). Such offset may correspond to the last seismic event on this fault, which is long enough to promote M6 or 7 class earthquakes (Feuillet et al., 2004).

6. Conclusions

Around the Lesser Antilles arc, the seafloor has been imaged by an extensive dataset of bathymetry and backscatter. Based on a detailed analysis of these data, we outlined several features allowing to define two distinct domains in the forearc on both sides of the Desirade fault: northwards, the Rough area with steep slopes incised by short canyons and large normal faults that control mid-slope and deep basins, and southwards, the Channelized area characterized by a gentle slope with sedimentary piled-up layers, incised by several long and sinuous canyons with pathways controlled by normal faults. In both areas, the main canyons are characterized by features which imply sediment transfers.

The sediments, which supply the basins, originate from the destabilization of the insular or accretionary wedge free-slopes and/or are carried through the canyons. The canyon heads are either confined on the slope or connected to the platforms and thus can collected sediment from shallow environments. During sea-level low-stands, the significant volume of sediment carried by the rivers, which drain the volcanic reliefs, appears not able to generate a sufficient erosion to form canyons, probably more shaped by regressive processes. However, paleo-canyons on the carbonate platform reveal that a connection may have exist between onshore and offshores systems. During sea-level high-stands, the material transported by the onshore systems appear to be stored on the platforms and mixed to the carbonate production. The fine fraction in suspension on the platform seems exported at the shelf-edge or to the canyon heads, probably by storms or density cascading. The canyons are also supplied by sediments which come from the destabilization of their walls. A part of the remobilized material settled into the canyon and are carried progressively to the basin by gravity currents which came

from upstream. The sediment transfer through the canyons is also controlled by the set of normal faults which can generating knickpoints or beheading of the canyons. Moreover, normal faults control the formation of mid-slope or deeper forearc basins. The depressions and grabens formed at the base of their scarp may trap sediments and form intermediate retention basins where the sediment is sorted before being transported in deeper basins.

Earthquakes on local faults or large subduction earthquakes can destabilize sediments, both generating slope failures in shallow or deep environments and flushing sediments accumulated in canyon heads or in intermediate basins. While some basins are connected to the shallow environments by the canyons (Desirade half graben, Desirade basin, Falmouth valley, Antigua valley and Martinique basin), others are isolated from terrestrial and shallow carbonate inputs (Falmouth half graben, Meduse basin, Tuda and Willoughby valleys and North and South Kalanina basins). Thus, these isolated basins are ideal core-sample targets to provide a paleoseismologic study.

TABLE AND FIGURE CAPTIONS

Table 1. Characterization of bathymetric data acquisition.

Table 2. EM12 acoustic classification

Table 3. Synthesis of the main geomorphologic features and inferred sedimentary processes in the two contrasting areas of the Lesser Antilles Arc

Figure 1. General map of the study area. A: Caribbean plate geodynamic and oceanographic settings. Black lines: Caribbean plate boundaries (Feuillet, 2000). Light blue: South-America rivers. Light red lines: oceanic ridges, Barracuda ridge (BR) and the Tiburon ridge (TR). Dark blue lines: turbiditic pathways from Orinoco delta (Deville et al., 2015). Dark red arrows: surface currents (Johns et al., 1998; Zhang et al., 2017), North Equatorial Current (NEC), Retroflection of the North Brazil Current (RNBC). **B:** Lesser Antilles Arc tectonic setting and adjacent structural domains. Light and dark gray: islands respectively from the inner arc and the outer arc (Mts: Montserrat; MG: Marie-Galante; FaB: Falmouth bank, BB: Bertrand bank, FB: Flandre bank, CB: Colombia bank, DBPB: Dien Bien Phu bank, AB: Amerique bank). Black: non-volcanic islands. Yellow stars: historical earthquakes, location from Feuillet et al. (2011a). Red triangles: active volcanoes. Brown lines: Debris avalanche deposits and submarine landslide from Deplus et al. (2001), Le Friant et al. (2004) and Brunet et al. (2016). Black line with ticks: fault systems from Feuillet et al. (2001, 2004).

Black line with triangles: accretionary prism frontal thrust and black dotted line: supposed inner prism limit. Blue lines: channels (dotted lines are supposed channels). Aseismic rides are highlighted by red lines and their subducted parts by red dotted lines. C: Longitudinal and transverse bathymetric profile across the Lesser Antilles Arc, location on Fig. 1B. Black dotted lines correspond to the Geomap bathymetry and black lines to the cruises bathymetry.

Figure 2. Raw backscatter data (left) and acoustic facies distribution according to the classification in Table 2. Location on Fig 1B, VLR: very low reflectivity; VHR: very high reflectivity.

Figure 3. Bathymetry, seafloor morphology, acoustic facies distribution and bathymetric profiles of the "Rough area". A: bathymetric map, location on Fig. 1B: shaded 100 m grid DEM; faults pattern from Feuillet et al. (2001, 2004). Blue line: watershed limit between the forearc and the backarc (blue arrows indicate the flowing directions). Red dotted line: subducting part pathway of Barracuda ridge. FB: Flandre Bank; BB: Bertrand bank; BT: Basse Terre; MB: Meduse Basin; W: Willoughby. B: Distribution of the six acoustic facies interpreted from backscatter data, in transparency on the hillshade. C: Bathymetric profiles along the main axis of the Antigua (1) and Désirade (2) troughs, from the carbonate shelf break to the basins, location on Fig. 3A. Three realms are distinguished: slope (respectively 15° and 10 ° for the Désirade and Antigua slope), valley from 6° to 2° and basin. D: Bathymetric profiles along and across the Willoughby (blue) and Bertrand (orange) thalwegs. The slope is divided in 5 segments: 1) canyon head; 2) convex-up incision; 3) fault bounded flat; 4) arc basement steepest slope; and 5) canyon mouth. The 5 km-wide cross profiles of these two canyons, the locations are indicating by orange dots and red dots on the longitudinal profiles.

Figure 4. 3D view of the "Rough" area, coupled with seismic profile AGUA26. Location on Fig. 3A. Vertical exaggeration: x5. Orange dotted lines: Bertrand and Willoughby canyons' axes. On the seismic profile, black lines correspond to main reflectors and red line to normal faults. BB: Bertrand Bank; FaB: Falmouth Bank.

Figure 5. Detailed bathymetric and seafloor morphology of the Desirade trough (on the left) and between Antigua and Grande-Terre and Bertrand/Falmouth spur (on the right). Location on Fig. 3A. A: bathymetric map: 100 m grid DEM with the slope-map in transparency, FB: Flandre Bank. The Desirade fault scarp is divided in 3 section: 1) eastern part; 2) middle part; and 3) western part. B: Backscatter data with very high reflectivity

(VHR) in black and very low reflectivity (VLR) in white. C: bathymetric map 100 m grid DEM with slope-map in transparency. Blue line: watershed limit, Red arrows: main displacement directions of remobilized sediments. White lines: slope failure scars. Zoomed bathymetric maps correspond to a 50 m-grid. FaB: Falmouth Bank; BB: Bertrand Bank. D: Backscatter data, same legend as for Fig. 5B.

Figure 6. Detailed slopes distribution around the La Desirade trough. A: DEM with slope-map in transparency, with mapping of the main canyons, white lines: slope failure scars, FB: Flandre Bank. B: Three bathymetric 500 m-spaced profiles spaced along the Desirade fault scarp; locations on Fig. 6A, with orange lines labeled « a » to « c » from upstream to downstream, 1-3 sections located on Fig. 5A. C: 500 m-spaced along-slope bathymetric profiles, perpendicular to main channel axes, labeled « d » to « i », locations on Fig. 6A. Areas surrounded by dotted lines lack well-defined channelized network. The three channel systems (Salines, Mussel and Bark) are in different blue shades, the lines superimposed by re dotted lines correspond to tributaries which canyon heads are confined on the slope. Black arrows highlight U-shape thalwegs. D: Bathymetric profile of the bedforms; section located on Fig. 6A.

Figure 7. Detailed bathymetry, seafloor morphology, and backscatter data of the Falmouth Half Graben. A: map view of a landslide location on Fig. 3A, with DEM with slope-map in transparency. B: raw backscatter data. C: interpretative backscatter map, legend on Fig. 3B. D: CAS-156 SB profiles located on 7A. On the interpreted profiles: Black lines: reflectors, red lines: erosion surfaces, red dotted lines: inferred erosion surfaces, blue surfaces: transparent unit associated to the landslide, and grey surfaces: the thick transparent layers.

Figure 8. Bathymetry, seafloor morphology, acoustic facies distribution and bathymetric profiles of the "Channelized area". A: bathymetric map of the channelized eastern area, 100 m grid shaded DEM, location on Fig. 1B. Light blue lines: river pathways, Dark blue line: watershed limit, Yellow lines: main canyon pathways, Black lines: canyons, White lines: gullies and rills. Normal fault mapping from Feuillet et al. (2001) and this study. BT: Basse-Terre, GB: Grande-Terre, MG: Marie-Galante, FB: Flandre Bank; CB: Colombie bank, NKB: North Kalanina Basin; SKB: South Kalanina Basin; DBP: Dien Bien Phu, c.: canyon. B: distribution of the 9 acoustic facies deduced from backscatter data (Fig. 2 and Table 2). C: Axial and transverse bathymetric profiles of the Arawak (orange), Melville Hall

(grey), and Bruce Castle (blue) canyons. Associated cross sections (downslope left and right) with same color as on longitudinal profiles, the locations are indicating by same color dots on the longitudinal profiles. Knp: Knickpoint.

Figure 9. Detailed bathymetry and seafloor morphology of Martinique forearc area and bathymetric profiles of canyons. A: 100 m grid DEM, with slope-map in transparency, location on Fig. 8A. Blue lines: river pathways (r.: river, G.r.: Grande rivière), Dark blue arrows: passes, Dark blue dotted lines: paleo-passes, Yellow lines: main canyons, Black dotted lines: paleo-canyons, White lines: slope failures scars. St Lucia channel is divided in three segments: S1: meandering segment; S2: abandoned meanders incised by active channel; S3: low-incise channel. Zone numbered 1: bedform set, zone numbered 2: slope failure, zone numbered 3: bedform set. The structural map of this area is in Appendix D. B: Axial and transverse bathymetric profiles of the canyons, left (L) and right (R) looking downslope; MTD: Mass transport deposit, Knp: knickpoint. The cross sections are labelled: a1 to a5 for Caravelle canyon, b1 to b5 for Robert canyon, c1 to c3 for Vauclin canyon, d1 for Paquemar canyon, e1 crossed the gullies of the upper Martinique canyon and f1 to f7 for St. Lucia canyon, blue arrows: terraces, red arrow: paleo-canyon.

Figure 10. 3D view of the Martinique forearc upper slope, coupled with seismic profile AGUA68. Location on Fig. 9A. Same legend as for Fig. 9. Vertical exaggeration: x5. Seismostratigraphic subdivision into three units: U1 blue, U2 black and U3 green.

Figure 11. Detailed bathymetry, seafloor morphology and main normal faults of the Dominica forearc area. A: 100 m grid DEM, with slope-map in transparency, location on Fig. 8A. Light blue lines: river pathways, Dark blue line: watershed limit, Yellow lines: main canyon pathways, Black lines: canyons, Black dotted lines: paleo-canyons, Red lines: Slope failure scars. B: Axial bathymetric profiles along Kalanina canyon (thalweg and flanks).

Figure 12. Detailed bathymetry, seafloor morphology and main normal fault of the Guadeloupe archipelago and Karukera spur. 100 m grid shaded DEM, location on Fig. 8A. Light blue lines: river pathways, Dark blue line: watershed limit, Yellow lines: main canyon pathways, Black lines: canyons. V: valley. Normal fault mapping from Feuillet et al. (2001).

Figure 13. Detailed bathymetry and detailed seafloor morphology of Arawak channel upper part and bounding slopes. A: 100 m grid shaded DEM, location on Fig. 12. Light

blue lines: river pathways (r.: river, GD: Grande Découverte), White arrows: carbonate platform passes, with the main passes labelled 1 and 2, Dark blue lines: offshore drainage system, Black dotted lines: paleo-canyon. Canyons originated from Banc des Vaisseaux slope are labeled a to f (associated to number when the canyon has several tributaries) and canyons originated from Marie-Galante slope are labeled 1 to 10 (associated to letter when the canyon has several tributaries). Grey surface: spreading of blocks, Red arrows: paleochannels, Orange surfaces: lobe mapped by Feuillet et al. (2004), Normal fault mapping from Feuillet et al. (2001). B: Raw backscatter data imaging the rill along the Grande Terre insular slope and blocks, located on Fig. 13A. C: CAS-139 SB profile of the Grande Terre insular slope, located on Fig. 13A. D: 50 m-grid DEM, with slope in transparency, of Arawak thalweg displaying patches of bedforms, location on Fig. 13A.

Figure 14. Gwad-gua1 Sub-Bottom profile of the Basse-Terre insular slope. Raw profile (up) located on Fig. 13A, and interpreted profile (down), considering a wave velocity of 1500 m Td. Red lines: normal faults, Yellow unit: Holocene transparent wedge, Orange unit: older stratified unit.

Figure 15. Detailed bathymetric map of Martinique Basin and bounding slopes. 100 m grid shaded DEM, location on Fig. 8A. Yellow lines: active channels, Black dotted lines: paleo-channels, labeled "a" to "f", Black lines: slope failure scars. The gullies network of the eastern side of the Martinique Basin is divided in three sub-group: 1, straight confined gullies and 2, long dendritic gullies. White dotted lines: rills. Two bathymetric profiles were made along the accretionary wedge slope of the Martinique Basin (AB) and in front of the Bruce Castle mouth (CD).

Figure 16. Synthetic view of the Lesser Antilles forearc, displaying main morphological features and active sediments pathways. Am. B.: Amerique Bank, DBP. B.: Dien Bien Phu Bank, B.B.: Bertrand Bank, Fa.B.: Falmouth Bank, SK. B.: South Kalanina Basin, NK. B.: North Kalanina Basin, B.: Basin, H.G.: Half Graben, V.: Valley, Fa. V.: Falmouth Valley, Tu V.: Turtle Valley, Wi V.: Willoughby Valley.

Appendix A. Navigation grids of the DEMs used in the GIS.

Appendix B. Longitudinal and transversal bathymetric profiles across the Lesser Antilles Arc.

Appendix C. Detailed bathymetry, seafloor morphology and bathymetric profiles of the Meduse Basin. White lines: landslide scars

Appendix D. Structural map of the Martinique forearc area, bathymetry details in Fig. 13A, and bathymetric profiles along the AA', BB' and CC' lines.

Appendix E. Axial and transverse bathymetric profiles of main thalwegs east of the Amerique and Dien Bien Phu banks. Canyon flanks (North and South) and thalweg (red lines on the map) bathymetric profiles of DBP1 and Kalanina canyons; and bathymetric profiles of three paleo-canyons in between (red dotted lines on the map). Knp: knickpoints: located on the map by black arrow.

ACKNOWLEDGMENTS

We thank the GENAVIR captains, officers and crew of R/V Pourquoi PAS? (IFREMER) and scientific cruise party. We thank also the AGUADOMAR, CARAVAL, SISMANTILLES2, GWADASEIS and BATHYSAINTES scientific parties for providing us with geophysical data. We are grateful to Institut de Physique du Globe de Paris, for PhD thesis funding, and to the French ANR CARQUAKES (contract number ANR-17-CE3-0006) and LABEX UnivEarthS project and the CNRS-INSU for financial support. We thank Ángel Puga-Bernabéu and anonymous reviewer for their constructive comments which helped to improve the manuscript.

REFERENCES

Aguilar, I., Sabatier, P., Beck, C., Audemard, F., Crouzet, C., Urbani, F., Campos, C., 2017. Calculation of the reservoir age from organic and carbonate fractions of sediments in the Gulf of Cariaco (Caribbean Sea). Quaternary Geochronology. 38, 50-60.

Andreieff, P., Bouysse, P., Westercamp, D., 1979. Reconnaissance géologique de l'arc insulaire des Petites Antilles. Résultats d'une campagne à la mer de prélèvements de roches entre Sainte-Lucie et Anguilla (Arcante 1). Bull. BRGM. *2*, 227-270.

Andresen, N., Reijmer, J.J.G., Droxler, A.W., 2003. Timing and distribution of calciturbidites around a deeply submerged carbonate platform in a seismically active setting (Pedro Bank, Northern Nicaragua Rise, Caribbean Sea). International Journal of Earth Sciences. 92, 573-592.

Babonneau, N., Delacourt, C., Cancouët, R., Sisavath, E., Bachèlery, P., Mazuel, A., Jorry, S.J., Deschamps, A., Ammann, J., Villeneuve, N., 2013. Direct sediment transfer from land to deep-sea: Insights into shallow multibeam bathymetry at La Réunion Island. Marine Geology. 346, 47-57.

Bangs, N.L., Christeson, G.L., Shipley, T.H., 2003. Structure of the Lesser Antilles subduction zone backstop and its role in a large accretionary system. J. Geophys. Res. 108(B7), 2358.

Bazin, S., Feuillet, N., Duclos, C., Crawford, W., Nercessian, A., Bengoubou-Valérius, M., Beauducel, F., Singh, S.C., 2010. The 2004–2005 Les Saintes (French West Indies) seismic aftershock sequence observed with ocean bottom seismometers. Tectonophysics. 489, 91-103.

Beck, C., Ogawa, Y., Dolan, J., 1990. Eocene paleogeography of the southeastern Caribbean, relations between sedimentation on the Atlantic abyssal plain at site 672 and evolution of the South America margin, in: Moore, J.C., Mascle, A., et al., 1990. Proceedings of the Ocean Drilling Program, Scientific Results, Vol. 110. pp. 7-15.

Beck, C., Reyss, J.-L., Leclerc, F., Moreno, E., Feuillet, N., Barrier, L., Beauducel, F., Boudon, G., Clement, V., Deplus, C., Gallou, N., Lebrun, J.-F., Le Friant, A., Nercessian, A., Paterne, M., Pichot, T., Vidal, C., 2012. Identification of deep subaqueous co-seismic scarps through specific coeval sedimentation in Lesser Antilles: implication for seismic hazard. Nat. Hazards Earth Syst. Sci. 12, 1755-1767.

Bénâtre, G., 2018. Sismotectonique du Prisme de la Barbade. Rapport de stage Master 2. pp. 32.

Bernard, P., Lambert, J., 1988. Subduction and seismic hazard in the northern Lesser Antilles: revision of the historical seismicity. Bulletin of the Seismological Society of America. 78(6), 1965-1983.

Boudon, G., Le Friant, A., Komorowski, J.-C., Deplus, C., Semet, M.P., 2007. Volcano flank instability in the Lesser Antilles Arc: Diversity of scale, processes, and temporal recurrence. J. Geophys. Res. 112, B08205.

Bourget, J., Zaragosi, S., Ellouz-Zimmermann, N., Mouchot, N., Garlan, T., Schneider, J.-L., Lanfumey, V., Lallemant, S., 2011. Turbidite system architecture and sedimentary processes along topographically complex slopes: the Makran convergent margin. Sedimentology. 58, 376-406.

Bouysse, P., Guennoc, P., 1983. Donnees sur la structure de l'arc insulaire des Petites Antilles, entre Ste-Lucie et Anguilla. Marine Geology. 53, 131-166.

Bouysse, P., Baubron, J.C., Richard, M.A., Maur, R.C., Andreieff, P., 1985. Evolution de la terminaison nord de l'arc interne des Petites Antilles au Plio-Quaternaire. Bulletin de la Société Géologique de France. 1(2), 181-188.

Bouysse, P., Mascle, A., 1994. Sedimentary basins and petroleum plays around the French Antilles. In Hydrocarbon and Petroleum Geology of France. Springer, Berlin, Heidelberg, 1994. 431-443.

Bouysse, P., Westercamp, D., 1990. Subduction of Atlantic aseismic ridges and Late Cenozoic evolution of the Lesser Antilles island arc. Tectonophysics. 175, 349-380.

Brunet, M., Le Friant, A., Boudon, G., Lafuerza, S., Talling, P., Hornbach, M., Ishizuka, O., Lebas, E., Guyard, H., IODP Expedition 340 Science Party, 2016. Composition, geometry, and emplacement dynamics of a large volcanic island landslide offshore Martinique: From volcano flank-collapse to seafloor sediment failure?. Geochem. Geophys. Geosyst. 17(3), 699-724.

Cambers, G., 2005. Caribbean Islands, coastal ecology and geomorphology. In M. L. Schwartz (Ed.), Encyclopedia of coastal science (pp. 221-226). Dordrecht: Springer. ISBN 978-1-4020-1903-6.

Canals, M., Puig, P., de Madron, X.D., Heussner, S., Palanques, A., Fabres, J., 2006. Flushing submarine canyons. Nature. 444, 354-357.

Capet, X., Chamley, H., Beck, C., Holtzapffel, T., 1990. Clay mineralogy of Sites 671 and 672, Barbados Ridge Accretionary Complex and Atlantic Abyssal Plain: paleoenvironmental and diagenetic implications. In Proceedings of the Ocean Drilling Program, Scientific Results. 110. 85-96.

Carey, S.N., Sigurdsson, H., 1980. The Roseau Ash: deep-sea tephra deposits from a major eruption on Dominica, Lesser Antilles Arc. Journal of Volcanology and Geothermal Research. 7, 67-86.

Carey, S., Sigurdsson, H., 1984. A model of volcanogenic sedimentation in marginal basins. Geological Society, London, Special Publications. 16, 37-58.

Carn, S.A., Watts, R.B., Thompson, G., Norton, G.E., 2004. Anatomy of a lava dome collapse: the 20 March 2000 event at Soufrière Hills Volcano, Montserrat. Journal of Volcanology and Geothermal Research. 131(3-4), 241-264.

Chiang, C.-S., Yu, H.-S., 2006. Morphotectonics and incision of the Kaoping submarine canyon, SW Taiwan orogenic wedge. Geomorphology. 80, 199-213.

Clark, P., Dyke, A., Shakun, J.D., Carlson, A. E., Clark, J., Wohlfarth, B., Mitrovica J.X., Hostetler S.W., McCabe, A.M., 2009. The last glacial maximum. Science. 325(5941), 710-714.

Collot, J. Y., Ratzov, G., Silva, P., Proust, J. N., Migeon, S., Hernandez, M. J., .Michaud, F., Pazmino, A., Barba Castillo, D., Alvarado, A., Khumara, S., 2019. The Esmeraldas Canyon: A Helpful Marker of the Pliocene-Pleistocene Tectonic Deformation of the North Ecuador-Southwest Colombia Convergent Margin. Tectonics, 38(8), 3140-3166.

De Min, L., 2014. Sismo-stratigraphie multi-échelles d'un bassin avant-arc : Le Bassin de Marie-Galante, Petites Antilles. PhD Thesis, Université des Antilles et de Guyane. pp. 360.

De Min, L., Lebrun, J.-F., Cornée, J.-J., Münch, P., Léticée, J.L., Quillévéré, F., Melinte-Dobrinescu, M., Randrianasolo, A., Marcaillou, B., Zami, F., 2015. Tectonic and sedimentary architecture of the Karukéra spur: A record of the Lesser Antilles fore-arc deformations since the Neogene. Marine Geology. 363, 15-37.

DeMets, C., Jansma, P.E., Mattioli, G.S., Dixon, T.H., Farina, F., Bilham, R., Calais, E., Mann, P., 2000. GPS geodetic constraints on Caribbean-North America Plate Motion. Geophys. Res. Lett. 27, 437-440.

Deng, J., Sykes, L.R., 1995. Determination of Euler pole for contemporary relative motion of Caribbean and North American plates using slip vectors of interplate earthquakes. Tectonics. 14, 39-53.

Deplus, C., Le Friant, A., Boudon, G., Komorowski, J.-C., Villemant, B., Harford, C., Ségoufin, J., Cheminée, J.-L., 2001. Submarine evidence for large-scale debris avalanches in the Lesser Antilles Arc. Earth and Planetary Science Letters. 192, 145-157.

Deville, E., Mascle, A., Callec, Y., Huyghe, P., Lallemant, S., Lerat, O., Mathieu, X., Padron de Carillo, C., Patriat, M., Pichot, T., Loubrieux, B., Granjeon, D., 2015. Tectonics and sedimentation interactions in the east Caribbean subduction zone: An overview from the Orinoco delta and the Barbados accretionary prism. Marine and Petroleum Geology. 64, 76-103.

Deville, E., Mascle, A., 2012. The Barbados Ridge: A mature accretionary wedge in front of the Lesser Antilles active margin. In Regional Geology and Tectonics: Principles of Geologic Analysis. Elsevier. 583-607.

Deville, É., Guerlais, S.H., Lallemant, S., Schneider, F., 2010. Fluid dynamics and subsurface sediment mobilization processes: an overview from Southeast Caribbean: Fluid dynamics and subsurface sediment mobilization processes. Basin Research. 22, 361-379.

Deville, E., Battani, A., Griboulard, R., Guerlais, S., Herbin, J.P., Houzay, J.P., Muller, C., Prinzhofer, A., 2003. The origin and processes of mud volcanism: new insights from Trinidad. Geological Society, London, Special Publications. 216(1), 475-490.

Dimego, G.J., Bosart, L.F., Endersen, G.W., 1976. An examination of the frequency and mean conditions surrounding frontal incursions into the Gulf of Mexico and Caribbean Sea. Monthly Weather Review. 104(6), 709-718.

Domzig, A., Gaullier, V., Giresse, P., Pauc, H., Déverchère, J., Yelles, K., 2009. Deposition processes from echo-character mapping along the western Algerian margin (Oran–Tenes), Western Mediterranean. Marine and Petroleum Geology. 26, 673-694.

Dorel, J., 1981. Seismicity and seismic gap in the Lesser Antilles arc and earthquake hazard in Guadeloupe. Geophysical Journal International. 67, 679-695.

Dugan, B., Flemings, P.B., 2000. Overpressure and fluid flow in the New Jersey continental slope: Implications for slope failure and cold seeps. Science. 289(5477), 288-291.

Durand, F., Augris, C., Castaing, P., 1998. Les cyclones David et Allen en Martinique : origine probable des mégarides sur le plateau externe oriental. Comptes Rendus de l'Académie des Sciences-Series IIA-Earth and Planetary Science. 326(12), 863-868.

Embley, R. W., Ewing, J. I., Ewing, M., 1970. The Vidal deep-sea channel and its relationship to the Demerara and Barracuda abyssal plains. In Deep Sea Research and Oceanographic Abstracts. Elsevier. 17(3), 539-552

Evain, M., Galve, A., Charvis, P., Laigle, M., Kopp, H., Bécel, A., Weinzierl, W., Hirn, A., Flueh, E.R., Gallart, J., 2013. Structure of the Lesser Antilles subduction forearc and backstop from 3D seismic refraction tomography. Tectonophysics. 603, 55-67.

Exon, N., Hill, P., Mitchell, C., Post, A., 2005. Nature and origin of the submarine Albany canyons off southwest Australia. Australian Journal of Earth Sciences. 52, 101-115.

Fauquembergue, K., Ducassou, E., Mulder, T., Hanquiez, V., Pereira, M.-C., Poli, E., Borgomano, J., 2018. Genesis and growth of a carbonate Holocene wedge on the northern Little Bahama Bank. Marine and Petroleum Geology. 96, 602-614.

Ferguson, I.J., Westbrook, G.K., Langseth, M.G., Thomas, G.P., 1993. Heat flow and thermal models of the Barbados Ridge accretionary complex. Journal of Geophysical Research: Solid Earth. 98(B3), 4121-4142.

Feuillard, M., 1985. Macrosismicité de la Guadeloupe et de la Martinique. Observatoire volcanologique de la Soufrière (Guadeloupe)

Feuillet, N., 2000. Sismotectonique des Petites Antilles : Liaison entre activité sismique et volcanique. PhD Thesis, University of Paris 7. pp. 283.

Feuillet, N., Beauducel, F., Tapponnier, P., 2011a. Tectonic context of moderate to large historical earthquakes in the Lesser Antilles and mechanical coupling with volcanoes. J. Geophys. Res. 116, B10308.

Feuillet, N., Beauducel, F., Jacques, E., Tapponnier, P., Delouis, B., Bazin, S., Vallée, M., King, G.C.P., 2011b. The Mw = 6.3, November 21, 2004, Les Saintes earthquake (Guadeloupe): Tectonic setting, slip model and static stress changes. J. Geophys. Res. 116, B10301.

Feuillet, N., Leclerc, F., Tapponnier, P., Beauducel, F., Boudon, G., Le Friant, A., Deplus, C., Lebrun, J.-F., Nercessian, A., Saurel, J.-M., Clément, V., 2010. Active faulting induced by slip partitioning in Montserrat and link with volcanic activity: New insights from the 2009 GWADASEIS marine cruise data. Geophysical Research Letters. 37(19).

Feuillet, N., Manighetti, I., Tapponnier, P., 2001. Extension active perpendiculaire à la subduction dans l'arc des Petites Antilles (Guadeloupe, Antilles françaises). Comptes Rendus de l'Académie des Sciences-Series IIA-Earth and Planetary Science. 333, 583-590.

Feuillet, N., Manighetti, I., Tapponnier, P., Jacques, E., 2002. Arc parallel extension and localization of volcanic complexes in Guadeloupe, Lesser Antilles. J. Geophys. Res. 107, 2331.

Feuillet, N., Tapponnier, P., Manighetti, I., Villemant, B., King, G.C.P., 2004. Differential uplift and tilt of Pleistocene reef platforms and Quaternary slip rate on the Morne-Piton normal fault (Guadeloupe, French West Indies). J. Geophys. Res. 109, B02404.

Feuillet, N., 2016, CASEIS cruise, RV Pourquoi pas ?, DOI: 10.17600/16001800

Feuillet, N., 2009, GWADASEIS cruise, RV Le Suroît, DOI: 10.17600/9020020

Green, A., Uken, R., 2008. Submarine landsliding and canyon evolution on the northern KwaZulu-Natal continental shelf, South Africa, SW Indian Ocean. Marine Geology. 254, 152-170.

Greene, H.G., Maher, N.M., Paull, C.K., 2002. Physiography of the Monterey Bay National Marine Sanctuary and implications about continental margin development. Marine Geology. 181, 55-82.

Gröger, M., Henrich, R., Bickert, T., 2003. Glacial–interglacial variability in lower North Atlantic deep water: inference from silt grain-size analysis and carbonate preservation in the western equatorial Atlantic. Marine Geology. 201, 321-332.

Hart, K., Carey, S., Sigurdsson, H., Sparks, R.S.J., Robertson, R.E.A., 2004. Discharge of pyroclastic flows into the sea during the 1996–1998 eruptions of the Soufrière Hills volcano, Montserrat. Bulletin of Volcanology. 66(7), 599-614.

Heezen, B. C., Ewing, W. M., 1952. Turbidity currents and submarine slumps, and the 1929 Grand Banks [Newfoundland] earthquake. American journal of Science. 250(12), 849-873.

Hough, S. E., 2013, Spatial variability of "Did You Feel It?" intensity data: Insights into sampling biases in historical earthquake intensity distributions. Bulletin of the Seismological Society of America. 103(5), 2767-2781.

Iacono, C.L., Sulli, A., Agate, M., Presti, V.L., Pepe, F., Catalano, R., 2011. Submarine canyon morphologies in the Gulf of Palermo (Southern Tyrrhenian Sea) and possible implications for geo-hazard. Mar Geophys Res. 32, 127.

Jo, A., Eberli, G.P., Grasmueck, M., 2015. Margin collapse and slope failure along southwestern Great Bahama Bank. Sedimentary geology. 317, 43-52.

Johns, W.E., Lee, T.N., Beardsley, R.C., Candela, J., Limeburner, R., Castro, B., 1998. Annual cycle and variability of the North Brazil Current. Journal of Physical Oceanography. 28, 103-128.

Johns, W.E., Townsend, T.L., Fratantoni, D.M., Wilson, W.D., 2002. On the Atlantic inflow to the Caribbean Sea. Deep Sea Research Part I. Oceanographic Research Papers. 49, 211-243.

Jorry, S.J., Droxler, A.W., Francis, J.M., 2010. Deepwater carbonate deposition in response to re-flooding of carbonate bank and atoll-tops at glacial terminations. Quaternary Science Reviews. 29, 2010-2026.

Lai, S.Y.J., Gerber, T.P., Amblas, D., 2016. An experimental approach to submarine canyon evolution: experimental submarine canyon evolution. Geophysical Research Letters. 43, 2741-2747.

Laigle, M., Becel, A., de Voogd, B., Sachpazi, M., Bayrakci, G., Lebrun, J.-F., Evain, M., 2013. Along-arc segmentation and interaction of subducting ridges with the Lesser Antilles Subduction forearc crust revealed by MCS imaging. Tectonophysics. 603, 32-54.

Lapuyade, J., 2015. Transferts sédimentaires sur une pente carbonatée moderne : Le lobe de la pente occidentale du Grand Banc des Bahamas. Rapport de stage Master 2, pp. 40.

Lastras, G., Arzola, R.G., Masson, D.G., Wynn, R.B., Huvenne, V.A.I., Hühnerbach, V., Canals, M., 2008. Geomorphology and sedimentary features in the Central Portuguese submarine canyons, Western Iberian margin. Geomorphology. 103, 310-329.

Laursen, J., Normark, W.R., 2002. Late Quaternary evolution of the San Antonio Submarine Canyon in the central Chile forearc (33 S). Marine Geology. 188, 365-390.

Le Friant, A., Boudon, G., Deplus, C., Villemant, B., 2003. Large-scale flank collapse events during the activity of Montagne Pelée, Martinique, Lesser Antilles. Journal of Geophysical Research: Solid Earth. 108(B1).

Le Friant, A., Harford, C.L., Deplus, C., Boudon, G., Sparks, R.S.J., Herd, R.A., Komorowski, J.C., 2004. Geomorphological evolution of Montserrat (West Indies): importance of flank collapse and erosional processes. Journal of the Geological Society. 161, 147-160.

Le Friant, A., Lock, E.J., Hart, M.B., Boudon, G., Sparks, R.S.J., Leng, M.J., Smart, C.W., Komorowski, J.C., Deplus, C., Fisher, J.K., 2008. Late Pleistocene tephrochronology of marine sediments adjacent to Montserrat, Lesser Antilles volcanic arc. Journal of the Geological Society. 165, 279-289.

Leclerc, F., Feuillet, N., Cabioch, G., Deplus, C., Lebrun, J.F., Bazin, S., Beauducel, F., Boudon, G., LeFriant, A., De Min, L., Melezan, D., 2014. The Holocene drowned reef of Les Saintes plateau as witness of a long-term tectonic subsidence along the Lesser Antilles volcanic arc in Guadeloupe. Marine Geology. 355, 115-135.

Leclerc, F., Feuillet, N., Deplus, C., 2016. Interactions between active faulting, volcanism, and sedimentary processes at an island arc: Insights from Les Saintes channel, Lesser Antilles arc: faulting, volcanism, and turbidity systems. Geochem. Geophys. Geosyst. 17, 2781-2802.

Leclerc, F., Feuillet, N., Perret, M., Cabioch, G., Bazin, S., Lebrun, J.-F., Saurel, J.M., 2015. The reef platform of Martinique: Interplay between eustasy, tectonic subsidence and volcanism since Late Pleistocene. Marine Geology. 369, 34-51.

Lehu, R., Lallemand, S., Hsu, S.-K., Babonneau, N., Ratzov, G., Lin, A.T., Dezileau, L., 2015. Deep-sea sedimentation offshore eastern Taiwan: Facies and processes characterization. Marine Geology. 369, 1-18.

Lindsay, J.M., Stasiuk, M.V., Shepherd, J.B., 2003. Geological history and potential hazards of the late-Pleistocene to Recent Plat Pays volcanic complex, Dominica, Lesser Antilles. Bulletin of Volcanology. 65, 201-220.

Maslin, M., Wc, L., Mikkelsen, N., Vilela, C., Haq, B., 1998. Sea-level–and gas-hydrate–controlled catastrophic sediment failures of the Amazon Fan. Geology. 26(12), 1107-1110.

McAdoo, B.G., Orange, D.L., Silver, E.A., McIntosh, K., Abbott, L., Galewsky, J., Kahn, L., Protti, M., 1996. Seafloor structural observations, Costa Rica Accretionary Prism. Geophys. Res. Lett. 23, 883-886

Micallef, A., Mountjoy, J.J., 2011. A topographic signature of a hydrodynamic origin for submarine gullies. Geology. 39, 115-118.

Micallef, A., Mountjoy, J.J., Barnes, P.M., Canals, M., Lastras, G., 2014. Geomorphic response of submarine canyons to tectonic activity: Insights from the Cook Strait canyon system, New Zealand. Geosphere. 10, 905-929.

Moore, J.C., Mascle, A., Taylor, E., Andreieff, P., Alvarez, F., Barnes, R., Clark, M., 1988. Tectonics and hydrogeology of the northern Barbados Ridge: results from Ocean Drilling Program Leg 110. Geological Society of America Bulletin. 100(10), 1578-1593.

Montenat, C., Barrier, P., Hibsch, C., 2007, Seismites: An attempt at critical analysis and classification. Sedimentary Geology. 196(1-4), 5-30.

Mountjoy, J.J., Barnes, P.M., Pettinga, J.R., 2009. Morphostructure and evolution of submarine canyons across an active margin: Cook Strait sector of the Hikurangi Margin, New Zealand. Marine Geology. 260, 45-68.

Mountjoy, J.J., Howarth, J.D., Orpin, A.R., Barnes, P.M., Bowden, D.A., Rowden, A.A., Schimel, A.C.G., Holden, C., Horgan, H.J., Nodder, S.D., Patton, J.R., Lamarche, G., Gerstenberger, M., Micallef, A., Pallentin, A., Kane, T., 2018. Earthquakes drive large-scale submarine canyon development and sediment supply to deep-ocean basins. Science Advances 4, eaar3748.

Mountjoy, J.J., Micallef, A., Stevens, C.L., Stirling, M.W., 2014. Holocene sedimentary activity in a non-terrestrially coupled submarine canyon: Cook Strait Canyon system, New Zealand. Deep Sea Research Part II: Topical Studies in Oceanography. 104, 120-133.

Mulder, T., Ducassou, E., Gillet, H., Hanquiez, V., Tournadour, E., Combes, J., Eberli, G.P., Kindler, P., Gonthier, E., Conesa, G., Robin, C., Sianipar, R., Reijmer, J.J.G., François, A., 2012. Canyon

morphology on a modern carbonate slope of the Bahamas: Evidence of regional tectonic tilting. Geology. 40, 771-774.

Mulder, T., Gillet, H., Hanquiez, V., Reijmer, J.J.G., Droxler, A.W., Recouvreur, A., Fabregas, N., Cavailhes, T., Fauquembergue, K., Blank, D.G., Guiastrennec, L., Seibert, C., Bashah, S., Bujan, S., Ducassou, E., Principaud, M., Conesa, G., Le Goff, J., Ragusa, J., Busson, J., Borgomano, J., 2019. Into the deep: A coarse-grained carbonate turbidite valley and canyon in ultra-deep carbonate setting. Marine Geology. 407, 316-333.

Mulder, T., Joumes, M., Hanquiez, V., Gillet, H., Reijmer, J.J.G., Tournadour, E., Chabaud, L., Principaud, M., Schnyder, J.S.D., Borgomano, J., Fauquembergue, K., Ducassou, E., Busson, J., 2017. Carbonate slope morphology revealing sediment transfer from bank-to-slope (Little Bahama Bank, Bahamas). Marine and Petroleum Geology. 83, 26-34.

Mullins, H.T., Hine, A.C., 1989. Scalloped bank margins: Beginning of the end for carbonate platforms? Geology. 17, 30-33.

Münch, P., Lebrun, J.-F., Cornée, J.-J., Thinon, I., Guennoc, P., Marcaillou, B.J., Begot, J., Bertrand, G., Berc, S.B.D., Biscarrat, K., Claud, C., Min, L.D., Fournier, F., Gailler, L., Graindorge, D., Léticée, J.-L., Marie, L., Mazabraud, Y., Melinte-Dobrinescu, M., Moissette, P., Quillévéré, F., Verati, C., Randrianasolo, A., 2013. Pliocene to Pleistocene carbonate systems of the Guadeloupe archipelago, French Lesser Antilles: a land and sea study (the KaShallow project). Bulletin de la Société Géologique de France. 184, 99-110.

Noda, A., TuZino, T., Furukawa, R., Joshima, M., Uchida, J., 2008. Physiographical and sedimentological characteristics of submarine canyons developed upon an active forearc slope: The Kushiro Submarine Canyon, northern Japan. Geological Society of America Bulletin. 120, 750-767.

Normandeau, A., Lajeunesse, P., St-Onge, G., Bourgault, D., Drouin, S.S.-O., Senneville, S., Bélanger, S., 2014. Morphodynamics in sediment-starved inner-shelf submarine canyons (Lower St. Lawrence Estuary, Eastern Canada). Marine Geology. 357, 243-255.

Paull, C.K., Ussler III, W., Caress, D.W., Lundsten, E., Covault, J.A., Maier, K.L., Xu, J., Augenstein, S., 2010. Origins of large crescent-shaped bedforms within the axial channel of Monterey Canyon, offshore California. Geosphere. 6, 755-774.

Picard, M., Schneider, J.-L., Boudon, G., 2006. Contrasting sedimentary processes along a convergent margin: the Lesser Antilles arc system. Geo-Mar Lett. 26, 397-410.

Pichot, T., Patriat, M., Westbrook, G.K., Nalpas, T., Gutscher, M.A., Roest, W.R., Deville, E., Moulin, M., Aslanian, D., Labineau, M., 2012. The Cenozoic tectonostratigraphic evolution of the Barracuda Ridge and Tiburon Rise, at the western end of the North America–South America plate boundary zone. Marine Geology. 303, 154-171.

Pindell, J., Kennan, L., Stanek, K.P., Maresch, W.V., Draper, G., 2006. Foundations of Gulf of Mexico and Caribbean evolution: eight controversies resolved. Geologica Acta, 4(1-2), 303-341.

Pinet, B., Lajat, D., Le Quellec, P., Bouysse, P., 1985. Structure of Aves Ridge and Grenada Basin from multichannel seismic data. In Géodynamique des caraïbes. Symposium. pp. 53-64.

Piper, D.J.W., Normark, W.R., 2009. Processes That Initiate Turbidity Currents and Their Influence on Turbidites: A Marine Geology Perspective. Journal of Sedimentary Research. 79, 347-362.

Poore, R.Z., Quinn, T.M., Verardo, S., 2004. Century-scale movement of the Atlantic Intertropical Convergence Zone linked to solar variability. Geophysical Research Letters. 31(12).

Pratson, L.F., Coakley, B.J., 1996. A model for the headward erosion of submarine canyons induced by downslope-eroding sediment flows. Geological Society of America Bulletin. 108, 225-234.

Principaud, M., 2015. Morphologie, architecture et dynamique sédimentaire d'une pente carbonatée moderne: le Great Bahama Bank (Bahamas). PhD Thesis, University of Bordeaux.

Principaud, M., Mulder, T., Hanquiez, V., Ducassou, E., Eberli, G.P., Chabaud, L., Borgomano, J., 2018. Recent morphology and sedimentary processes along the western slope of Great Bahama Bank (Bahamas). Sedimentology. 65, 2088-2116.

Prospero, J.M., Bonatti, E., Schubert, C., Carlson, T.N., 1970. Dust in the Caribbean atmosphere traced to an African dust storm. Earth and Planetary Science Letters. 9, 287-293.

Prospero, J.M., Collard, F.-X., Molinié, J., Jeannot, A., 2014. Characterizing the annual cycle of African dust transport to the Caribbean Basin and South America and its impact on the environment and air quality: African dust transport to South America. Global Biogeochemical Cycles. 28, 757-773.

Puga-Bernabéu, Á., Webster, J.M., Beaman, R.J., Guilbaud, V., 2011. Morphology and controls on the evolution of a mixed carbonate–siliciclastic submarine canyon system, Great Barrier Reef margin, north-eastern Australia. Marine Geology. 289, 100-116.

Puga-Bernabéu, Á., Webster, J.M., Beaman, R.J, Guilbaud, V., 2013. Variation in canyon morphology on the Great Barrier Reef margin, north-eastern Australia: The influence of slope and barrier reefs. Geomorphology. 191, 35-50.

Puig, P., Ogston, A.S., Mullenbach, B.L., Nittrouer, C.A., Parsons, J.D., Sternberg, R.W., 2004. Storm-induced sediment gravity flows at the head of the Eel submarine canyon, northern California margin. J. Geophys. Res. 109, C03019.

Rad, S., Louvat, P., Gorge, C., Gaillardet, J., Allègre, C.J., 2006. River dissolved and solid loads in the Lesser Antilles: New insight into basalt weathering processes. Journal of Geochemical Exploration. 88, 308-312.

Rad, S., Rivé, K., Vittecoq, B., Cerdan, O., Allègre, C.J., 2013. Chemical weathering and erosion rates in the Lesser Antilles: An overview in Guadeloupe, Martinique and Dominica. Journal of South American Earth Sciences. 45, 331-344.

Ratzov, G., Sosson, M., Collot, J.-Y., Migeon, S., 2012. Late Quaternary geomorphologic evolution of submarine canyons as a marker of active deformation on convergent margins: The example of the South Colombian margin. Marine Geology. 315, 77-97.

Rebesco, M., Neagu, R.C., Cuppari, A., Muto, F., Accettella, D., Dominici, R., Cova, A., Romano, C., Caburlotto, A., 2009. Morphobathymetric analysis and evidence of submarine mass movements in the western Gulf of Taranto (Calabria margin, Ionian Sea). Int. J. Earth Sci. 98, 791-805.

Reid, R.P., Carey, S.N., Ross, D.R., 1996. Late Quaternary sedimentation in the Lesser Antilles island arc. Geological Society of America Bulletin. 108, 78-100.

Rhein, M., Stramma, L., Krahmann, G., 1998. The spreading of Antarctic bottom water in the tropical Atlantic. Deep Sea Research Part I: Oceanographic Research Papers. 45, 507-527.

Robson, G. R., 1964, An earthquake catalogue for the eastern Caribbean, Bull. Seismol. Soc. Am., 54, 785-832.

Ryan, W.B.F., Carbotte, S.M., Coplan, J.O., O'Hara, S., Melkonian, A., Arko, R., Weissel, R.A., Ferrini, V., Goodwillie, A., Nitsche, F., Bonczkowski, J., Zemsky, R., 2009. Global Multi-Resolution Topography synthesis. Geochem. Geophys. Geosyst. 10(3).

Saffache, P., Marc, J.-V., Cospar, O., 2002. Les cyclones en Martinique : quatre siècles cataclysmiques. IBIS Rouge Editions, Martinique. pp. 197.

Saffache, P., Marc, J.-V., Huyghes-Belrose, V., 2003. Les cyclones en Guadeloupe : quatre siècles cataclysmiques. IBIS Rouge Editions, Martinique, pp. 276.

Schwartz, D.P., Coppersmith, K.J., 1984. Fault behavior and characteristic earthquakes: Examples from the Wasatch and San Andreas fault zones. Journal of Geophysical Research: Solid Earth. 89(B7), 5681-5698.

Seibert, C., 2019. Transferts sédimentaires et Grands séismes dans l'Arc des Petites Antilles, apport de la paléoseismologie en mer. PhD Thesis, Institut de Physique du Globe de Paris.

Shepherd, J. B. (1992), Comment on "Subduction and seismic hazard in the Lesser Antilles" by Pascal Bernard and Jérôme Lambert, Bull. Seismol. Soc. Am. 82(3), 1534-1543.

Shimazaki, K., Nakata, T., 1980. Time-predictable recurrence model for large earthquakes. Geophysical Research Letters. 7(4), 279-282.

Sigurdsson, H., Carey, S.N., 1981. Marine Tephrochronology and Quaternary Explosive Volcanism in the Lesser Antilles Arc. In Self, S., Sparks, R.S.J. (Eds.), Tephra Studies. Springer Netherlands, Dordrecht. pp. 255-280.

Sigurdsson, H., Sparks, R.S.J., Carey, S. t, Huang, T.C., 1980. Volcanogenic sedimentation in the Lesser Antilles arc. The Journal of Geology. 88, 523-540.

Stein, S., Engeln, J.F., Wiens, D.A., Fujita, K., Speed, R.C., 1982. Subduction seismicity and tectonics in the Lesser Antilles Arc. J. Geophys. Res. 87, 8642.

Speed, R. C., 1981. Geology of Barbados: implication for an accretionary origin. XXVIth Intern. Geol. Congr., Paris C-3; Oceanol. Acta. 4. 259-265

Stéphan, J. F., Mercier-de-Lepinay, B., Calais, E., Tardy, M., Beck, C., Carfantan, J. C., Olivet, J.L., Vila, J.M., Bouysse, P., Mauffret, A., Bourgois J., Thery, J. M., Tournon, J., Blanchet R., Dercourt J., 1990. Paleogeodynamic maps of the Caribbean: 14 steps from Lias to Present. Bull. Soc. Géol. Fr. 6(8), 6-919.

Stigall, J., Dugan, B., 2010. Overpressure and earthquake initiated slope failure in the Ursa region, northern Gulf of Mexico. J. Geophys. Res. 115, B04101.

Sykes, L.R., Ewing, M., 1965. The seismicity of the Caribbean region. Journal of Geophysical Research. 70(20), 5065-5074.

Symithe, S., Calais, E., de Chabalier, J.B., Robertson, R., Higgins, M., 2015. Current block motions and strain accumulation on active faults in the Caribbean: current caribbean kinematics. Journal of Geophysical Research: Solid Earth. 120, 3748-3774.

Tournadour, E., Mulder, T., Borgomano, J., Gillet, H., Chabaud, L., Ducassou, E., Hanquiez, V., Etienne, S., 2017. Submarine canyon morphologies and evolution in modern carbonate settings: The northern slope of Little Bahama Bank, Bahamas. Marine Geology. 391, 76-97.

Trofimovs, J., Fisher, J.K., Macdonald, H.A., Talling, P.J., Sparks, R.S.J., Hart, M.B., Smart, C.W., Boudon, G., Deplus, C., Komorowski, J.-C., Le Friant, A., Moreton, S.G., Leng, M.J., 2010. Evidence for carbonate platform failure during rapid sea-level rise; ca 14 000 year old bioclastic flow deposits in the Lesser Antilles: Voluminous bioclastic flow deposits, Lesser Antilles. Sedimentology. 57, 733-759.

Trofimovs, J., Talling, P.J., Fisher, J.K., Sparks, R.S.J., Watt, S.F.L., Hart, M.B., Smart, C.W., Le Friant, A., Cassidy, M., Moreton, S.G., Leng, M.J., 2013. Timing, origin and emplacement dynamics of mass flows offshore of SE Montserrat in the last 110 ka: Implications for landslide and tsunami hazards, eruption history, and volcanic island evolution: mass flows offshore of Montserrat. Geochem. Geophys. Geosyst. 14, 385-406.

Warne, A.G., Meade, R.H., White, W.A., Guevara, E.H., Gibeaut, J., Smyth, R. C., Tremblay, T., 2002. Regional controls on geomorphology, hydrology, and ecosystem integrity in the Orinoco Delta, Venezuela. Geomorphology. 44(3-4), 273-307.

Westbrook, G.K., Smith, M.J., Peacock, J.H., Poulter, M.J., 1982. Extensive underthrusting of undeformed sediment beneath the accretionary complex of the Lesser Antilles subduction zone. Nature. 300(5893), 625

Westbrook, G.K., Ladd, J.W., Buhl, P., Bangs, N., Tiley, G.J., 1988. Cross section of an accretionary wedge: Barbados Ridge complex. Geology. 16(7), 631-635.

Wilson, P.A., Roberts, H.H., 1995. Density cascading; off-shelf sediment transport, evidence and implications, Bahama Banks. Journal of Sedimentary Research. 65(1a), 45-56.

Woodworth, P.L., 2017. Seiches in the Eastern Caribbean. Pure and Applied Geophysics. 174, 4283–4312.

Wright, A., 1984, sediment distribution and depositional processes operating in the Lesser Antilles intraoceanic island-arc, Eastern Caribbean. Initial Reports of the Deep Sea Drilling Project. 78(AUG), 301-324.

Wynn, R.B., Stow, D.A., 2002. Classification and characterisation of deep-water sediment waves. Marine Geology. 192, 7-22.

Yu, H., Chin, M., Bian, H., Yuan, T., Prospero, J.M., Omar, A.H., Remer, L.A., Winker, D.M., Yang, Y., Zhang, Y., Zhang, Z., 2015. Quantification of trans-Atlantic dust transport from seven-year (2007–2013) record of CALIPSO lidar measurements. Remote Sensing of Environment. 159, 232-249.

Zahibo, N., Pelinovsky, E., Talipova, T., Rabinovich, A., Kurkin, A., Nikolkina, I., 2007. Statistical analysis of cyclone hazard for Guadeloupe, Lesser Antilles. Atmospheric Research. 84(1), 13-29.

Zhang, Y., Chiessi, C.M., Mulitza, S., Sawakuchi, A.O., Häggi, C., Zabel, M., Portilho-Ramos, R.C., Schefuß, E., Crivellari, S., Wefer, G., 2017. Different precipitation patterns across tropical South America during Heinrich and Dansgaard-Oeschger stadials. Quaternary Science Reviews. 177, 1-9.

Cruise	Vessel	Equipment	Investigated depth	Areas
AGUADOMAR (1999)	R/V ATALANTE	EM12	100 - 6000 m	Backarc and Forearc fro Lucia
DOI 10.17600/98010120		EM1000		
CARAVAL (2002)	R/V ATALANTE	Simrad EM12	100 - 6000 m	Backarc from Montserrat
DOI 10.17600/18000929				
SISMANTILLES2 (2007)	R/V ATALANTE	Simrad EM12	100 - 6000 m	Forearc and accretiona Antigua to Martinique
DOI 10.17600/7010020				
GWADASEIS (2009)	R/V LE SUROIT	EM300	20 - 4000 m	Arc from Saba to St. Luc
DOI 10.17600/9020020				
BATHYSAINTES (2011)	R/V POURQUOI PAS ?	seabat7111	30 - 200 m	Saintes insular shelf
		Seabat7150	200 - 1500 m	Saintes channel
DOI 10.17600/10030020	Le Pelican hydrographic launcher	EM3002	0 - 30 m	littoral area
LITTO 3D (2011)		LiDAR bathymetric	0 - 10 m	Platform of Martinique a

of Guadeloupe

CASEIS (2016)	R/V POURQUOI PAS ?	Reson 7150	500 - 7000 m	Forearc and accretiona Anguilla to St. Lucia

DOI
10.17600/16001800

Class	Legend	Raw data	Description	Location
Very High Reflectivity		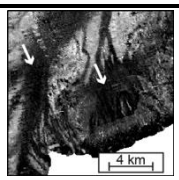	Heterogeneous, with patches	Very shallow areas, very steep slopes and some canyon's thalwegs
		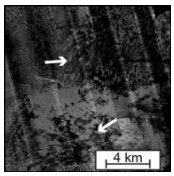	Heterogeneous, with mottled aspect	Between Antigua and Guadeloupe islands
High Reflectivity		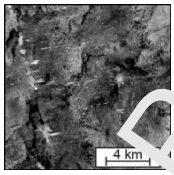	Heterogeneous, with patches	Shallow areas and some canyon's thalwegs
Medium Reflectivity		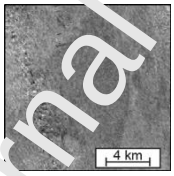	Heterogeneous, with patches	On the boundary of accretionary prism and forearc area, some canyon's thalwegs
		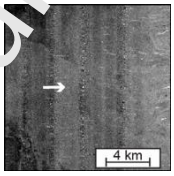	Homogeneous	On the upper part of insular slope in front of Martinique and Marie-Galante
Low Reflectivity		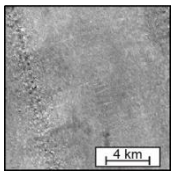	Heterogeneous, with patches	On the bottom of deep basins and in some parts of the slope in front of dominica
		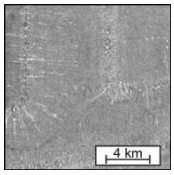	Homogeneous	On insular slope in front of Martinique and in Arawak valley

		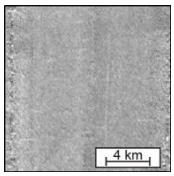	Homogeneous	On insular slope in front of Martinique
Very Low Reflectivity		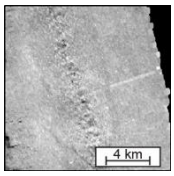	Heterogeneous, with patches	On the bottom of basins and on some parts of the slope in front of Dominica

Areas	Canyons	Slope failures	Connection with onshore systems
Rough Area	V-shaped to U-shaped dendritic canyons connected with the reef insular shelf break V-shaped straight canyons, with canyon head connected to shallow area or confined on the slope Willoughby and Bertrand canyons with a complex pathway controlled by faults	Hummocky and blocky deposits surrounded the carbonate platforms Scalloped morphology of the platform shelf break (*Mullins and Hine, 1989; Jo et al., 2015*) Landslide scars and associated MTD originating from the destabilization of the foothill of the accretionary wedge	No permanent river flow on the low lying and flat islands No connection exists with the rivers which run on the volcanic islands, whose mouths are located west of the water divide
Channelized Area	The canyon heads differ throughout the area: - Large canyon heads incising the carbonate platform of Martinique - On the insular slope of Dominica, downward coalescent rills and gullies - Arawak canyon collect all the rills, gullies and mature canyons which incised the shelf break of the surrounding insular slope of the Guadeloupe archipelago The canyon pathways are long and more or less sinuous, mainly controlled by normal faults (EW and N130°E) and disrupted by several knickpoints All canyons but the Bruce Castle canyon vanish on the slope	Huge blocky deposit downward the Guadeloupe platform On the insular slope Numerous landslide scars along the canyon walls and MTD settled in the bottom of the canyons	From Martinique: Galion river is the only one to flow westwards and is nowadays disconnected to the canyon head by a large carbonate platform and Holocene reef barriers. Small smooth incisions can be identified on the deeper carbonate platform upstream the Paquemar and Hardy canyon heads, they have likely connected the terrestrial and offshore system in the past From Guadeloupe: Large passes have developed at the mouth of the main rivers draining the highest reliefs of Basse-Terre. In front of the main river, an up to 45 m-thick transparent sedimentary wedge is identified

We do not have conflicts of interest to report

- Morpho-sedimentary study of Lesser Antilles forearc
- Two distinct morphological domains along the forearc (Rough and Channelized areas)

- Active sediment transfers through canyons and slope failures supply the deep basins
- Tectonic and sea-level fluctuations control the sediment transfers
- Isolated basins should mainly record co-seismic turbidites

Seafloor morphology and sediments transfers in the mixed carbonated-siliciclastic environment of the Lesser Antilles forearc along Barbuda and St. Lucia

C. Seibert

Université de Paris, Institut de physique du globe de Paris, CNRS, F-75005 Paris, France

Corresponding author : seibert@ipgp.fr

N. Feuillet

Université de Paris, Institut de physique du globe de Paris, CNRS, F-75005 Paris, France

G. Ratzov

Géoazur, Université de Nice Sophia-Antipolis, CNRS, Observatoire de la Côte d'Azur, 250 rue Albert Einstein, 06560 Valbonne, France

C. Beck

CNRS ISTerre, Université Savoie-Mont-Blanc, 73 376, Le Bourget du Lac, France

A. Cattaneo

IFREMER, Géosciences Marines, BP. 70, 29280 Plouzané, France